2-1-2014

Studying binary clathrate hydrate of hydrogen and deuterium using raman spectroscopy

Moaaz El.Ghazaly

The American University in Cairo

School of Sciences & Engineering

Studying Binary Clathrate Hydrate of Hydrogen and Deuterium Using Raman Spectroscopy

A Thesis submitted to

The Physics Graduate Program

In partial fulfillment of the requirements for the degree of

Master of Science

By

Moaaz A. El.Ghazaly

Supervisor: Prof. Salah El.Sheikh

Physics Department, The American University in Cairo

Co-Advisor: Dr. Lorenzo Ulivi

Institute of Complex Systems, National Research Center, Florence, Italy

July 2013

" رَبِّ أوزعنى أن أشكُرَ نِعمَتَكَ التى أنعَمتَ علىّ، وعلى والدىّ، وأن أعملَ صالحاً ترضاهُ، وأدخلنى برَحمَتِكَ فى عبادِكَ الصالحينْ "

النمل، 19

ACKNOWLEDGEMENTS

All praises and thanks to **Allah**, the most gracious the most merciful, for all his apparent and unapparent graces and favors.

Thanks to **my parents** for their continuous and unconditional support, patience, love and dedication. It was really impossible to go for this whole postgraduate study without your support. I will do my best to never let you down.

Thanks to **Prof. Salah El.Sheikh** not only for being a professional supervisor, but also for being a father. Your guidance, wisdom, support and kindness all together enlightened my career path as well as my personal life.

Thanks to **Prof. Lorenzo Ulivi** for giving me the opportunity of doing this research in his laboratory. It was truly an honor and a great experience to work with such talented, skilled experimentalist.

Thanks to **Prof. Milva Celli** for her patience and assistance during all whole research process. Your consultations and help with data analysis process were cornerstones for this study to be done.

Thanks to my dear friend **Mohamed Mousa** for the best accompany he supplied me with during our stay in Italy as well as at AUC. Our discussions concerning this research and your suggestions were so beneficial.

Thanks to my friend **Mohamed Zaghloul** for supporting me with all the required information about his own research and about Italy. It is my pleasure to know such a friendly colleague.

Thanks to all **my friends and colleges** in physics department at The American University in Cairo for having me with you and offering a friendly atmosphere. I'll never forget our happiest moments at room 1129.

Thanks to my **elder sister** for encouraging me to apply for the master's degree at AUC. I'm so blessed to have such a lovely, kind sister.

Thanks to my **younger sister** for inspiring me with her own faith, determination, patience and unlimited hope.

Thanks to my **brother** who helped me to prepare my first resume ever, and for his continuous support.

SPECIAL thanks to my lovely **fiancée**, **Aya**, for the wonderful days I'm living with you. You have already given me all the motivation to be a better person rather than to finalize this thesis.

TABLE OF CONTENTS

LIST OF FIGURES

LIST OF SYMBOLS & ABBREVIATIONS & UNITS

Symbols

$\boldsymbol{E}$	Electric Field
$\boldsymbol{P}$	Electric Dipole Moment
$\boldsymbol{\alpha}$	Polarizability of the molecule
$\boldsymbol{f_0}$	Initial Frequency
$\boldsymbol{\Delta f}$	Change in Frequency
$\boldsymbol{E_0}$	Electric Field Intensity
$\boldsymbol{t}$	Time
$\boldsymbol{\alpha_0}$	Polarizability before incident light
$\boldsymbol{q}$	Dimension Coordinate
$\boldsymbol{hv}$	Photon Energy
$\boldsymbol{h}$	Plank Constant
$\boldsymbol{E}$	Energy Level
$\boldsymbol{\Delta E}$	Difference between two Energy Levels
$\boldsymbol{\psi}$	Wave Function for a certain state
$\boldsymbol{dr}$	Spatial Element

a, c	Lattice Spacing
B_0	Rotational Constant
J	Rotational Quantum Number
I	Molecular Spin Quantum Number
T	Temperature
k_B	Boltzmann Constant
C	Speed of Light
n^o	Ortho Ratio
n^p	Para Ratio
υ	Vibrational State Quantum Number

Abbreviations

IR	Infrared Spectroscopy
NMR	Nuclear Magnetic Resonance
sI	First Structure
sII	Second Structure
sH	Hexagonal Structure
MTBE	Methyl Tertiary Butyl Ether
THF	Tetrahydrofuran
A.U	Arbitrary unit
CCD	Charge Coupled Device
SC	Small cage

MC Middle Cage

MOS Metal-Oxide Semiconductor Capacitor

Units

1 MPa = 10^{6} Pa

1 Kbar = 10^{3} bar

1 Bar = 10^{5} Pa

1 Å = 10^{-10} m

1 Cm^{-1} = 1.23984×10^{-4} eV

ABSTRACT

In the scene of the increasing global need to find a good manner to use hydrogen as a source of energy; this research stand as one of the promising methods to do so. Clathrate hydrates show a possible material to store hydrogen which is a clean fuel and exist in nature in large quantities at different places.

Clathrate hydrates are crystalline molecules with shape like ice, but have different crystal structure. Simply, applying high pressure and low temperature on water molecules will form Clathrate hydrate which represents a phase transition from water. About 6.4 trillion tones of methane-hydrates are found to be deep on ocean floor, which represent a significant source of energy just requires an efficient and economical method to be used.

Besides the importance of clathrates in terms of energy demands, this research participates in increasing the knowledge of fundamental physical and chemical processes in one of the important international research topics.

Raman spectroscopy has been performed on different samples of binary Clathrate hydrate of hydrogen and deuterium. Actually, we used Raman Spectroscopy because it is a powerful tool for investigating the molecular dynamics of the guest molecule inside the clathrate cages, in addition to estimating the occupancy number of molecules per cage.

The experimental part of this thesis was done at CNR, Florence, Italy, while the data analysis was carried out at Physics department, The American University in Cairo in the scene of scientific collaboration between the two institutions.

Chapter 1 : INTRODUCTION TO CLATHRATE HYDRATE

1.1 Clathrates and Clathrate hydrate.

Clathrates are compounds in which molecules of one component are physically trapped within the crystal structure of another. [1] Historically, it was believed that Clathrate compounds are kind of polymers in which the guest molecule is totally enclosed. However, it has been redefined as inclusion compounds in the form of host-guest system. The host molecules create a cavity, under some conditions, and the guest molecules are accommodated inside these cages. It is important to note that the formation of such molecules don't show any kind of chemical reactions or strong chemical bonds, however, it is a kind of phase transition process.

The Clathrate name was coined by H. M. Powell in 1948 after his work on analyzing the crystal structures of such compounds. The term "Clathrate" is derived from the Latin word "Clathratus" means "inside lattice".

Clathrates were discovered by Sir Humphrey Davy in 1810 when he noticed that a mixture of water and chlorine froze with more speed than the conventional water. [2] Such discovery was classified as a laboratory curiosity. Later on, clathrate molecules caused problems for the petroleum industry when engineers in 1930's encountered the formation of clathrate molecules inside the pipelines in a way that decreases the efficiency of transportation. Since then, more interest and

investigation have been given to clathrates. Because some clathrate molecules such as clathrate hydrate are promising energy sources, recent studies on clathrate hydrates are being carried on to fully understand the clathrate formation process and different structural parameters.

Indeed, one of the significant types of clathrates is the clathrate hydrate. Clathrate hydrates are crystalline water-based solids in which water is the host molecule that are forming polyhedral cages, of different geometry and size. Such cages are capable of trapping another guest molecule (gas or liquid) inside them to form the clathrate. Forming such a stabilized network requires a certain pressure and temperature. Without guest molecule, the clathrate hydrate lattice would not be stable, and will crystallize into ice structure or liquid water. The formation and decomposition of clathrate hydrates is not a chemical reaction, but it is a change of phase process. For example H_2, O_2, co_2, CH_4, Ar, Kr, N_2 are possible guest molecules that forms Clathrate hydrates. According to the pressure and temperature, hydrogen may form clathrates or diffuse in ordinary ice.

Clathrates usually have three crystal structures which are cubic sI and cubic sII, and hexagonal sH, forming two types of cages (small and large). The cages of guest molecules have the form of hexagons, squares or polyhedral with pentagon faces. The guest molecule controls the average radii of the cages. For the crystal sII, radii of cavities are about 3.95 A for the small cage and 4.33 for the large cage. The space group for this structure is Fd3m.

Two kinds of clathrates are possible hydrogen storage materials at different pressures and temperatures. The simple hydrogen clathrate hydrates which are formed of H_2o and H_2 needs pressure of about 2000 bar at room temperature to be formed. While binary clathrate with tetrahydrofuran THF is about to store hydrogen at lower pressure. Both kinds have sII crystal structure.

Successive research shows that clathrate hydrates have lots of interesting properties that put it along with hot topics of research in physics and material science. One of these applications is that clathrate hydrates are possible materials for hydrogen storage. Scientists tried for decades to use hydrogen as fuel because H_2 has higher mass based combustion energy than any other fuel. However, using hydrogen as a fuel with energy densities comparable to other fuels is not easy in terms of the economic point of view. So that, clathrate hydrates may solve such problem because it show lots of advantages. One of the advantages is that the host material is water which is economic. In addition, no chemical reaction is required for releasing hydrogen from the clathrate, however, increasing the temperature is sufficient to destroy clathrate and release hydrogen. On the contrary, the only and apparent disadvantage of clathrates is the relatively high pressure (200 MPa at 273 K) necessary for formation, which requires more search for clathrates with more convenient conditions. [3]

In addition to the storage capability, clathrate molecules exist in nature with a large amount, which represent a huge energy reservoir. Scientists found that there are about 6.4 trillion tones of methane-hydrates exist deep on ocean floor. This huge energy reservoir is expected to replace the fossil fuel in future, so that more investigation is significant to fully understand the formation and properties of clathrate molecules.

Moreover, investigating clathrates participate into the basic literature of physics and chemistry as it reveals one of the interesting processes.

Scientists have used different tools to investigate clathrates including NMR, neutron scattering, IR, and Raman spectroscopy. In this research, Raman spectroscopy has been performed to investigate clathrate hydrate. Indeed, Raman

spectroscopy has been chosen because it is a powerful tool that gives valuable information about dynamics of guest molecules inside polyhedral cages, in addition to the evaluation of occupancy number of guest molecules for each cage.

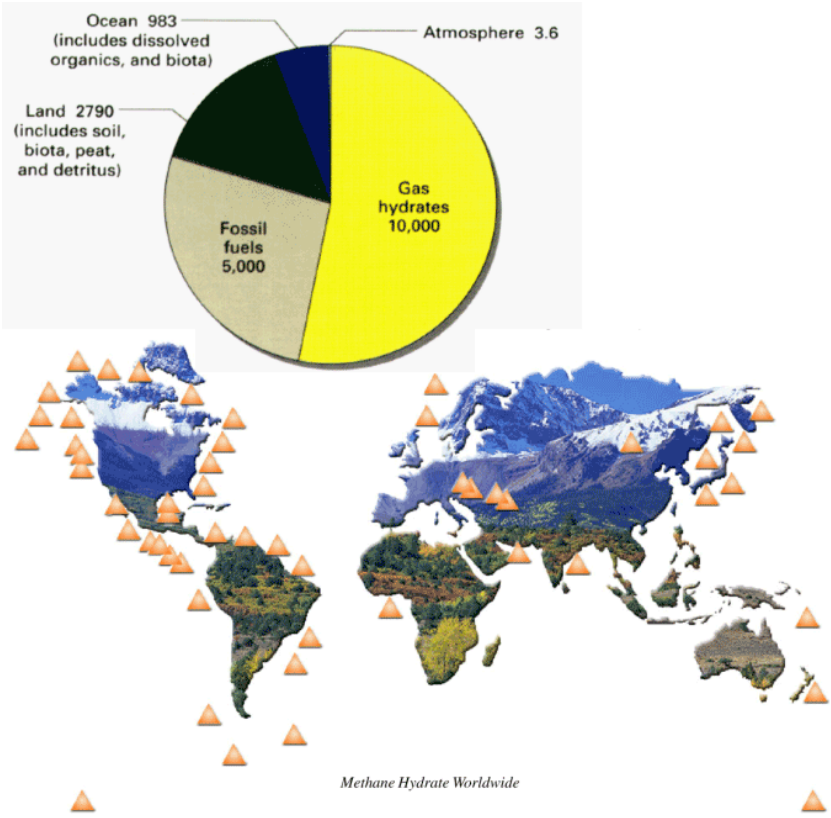

Figure 1.1: Distribution of Methane Clathrate Resources Worldwide. From Los Alamos National Laboratory [4]

1.2 Raman Spectroscopy

It is a technique that investigates the vibrational and rotational modes for molecules and atoms. The process is simply an interaction between an incident electromagnetic radiation, typically LASER, with frequency lies in the visible region and the material under investigation. Due to the interaction between the incident beam and molecular vibrations and phonons, the energy of the LASER beam shifts up or down. This energy shift gives information about the vibrational and rotational modes. The theory of Raman spectroscopy can be explained either by classical or quantum point of view.

1.1.1 Classical Theory of Raman Scattering

The classical explanation of Raman scattering was conducted by G. Placzek. However classical theory is not able to explain all features of Raman scattering, it can correctly predict frequency dependence and selection rules. [5]

As the incident electromagnetic radiation interacts with the molecule, the electric field associated with the electromagnetic radiation will induce a dipole moment (P) at the molecule. The classical explanation is considering the relation between the electric field of the incident radiation and this induced electric dipole moment of a molecule.

This induced dipole moment oscillates with a certain frequency, and Polarizability changes with vibrations. As a result, the emitted beam will have frequency combination between the frequency dependence of Polarizability and frequency dependence of incident beam. [5]

1.2.1 Quantum Theory of Raman Scattering

According to quantum mechanics, when an electromagnetic radiation interacts with atoms and molecules, an inelastic photon scattering will occur. This means that as a result of collision, molecules would acquire an amount of energy from the incident photon, and consequently will be excited to a higher virtual vibrational or rotational energy state. After that, the molecule would decay to a final stable energy state which is higher than the original energy state, and the photon will recoil with frequency lower than the frequency of the incidence. This frequency shift between the scattered photon gives information about the molecule vibrational and rotational behavior as shown in figure (1.2).
In addition, the reverse process is also possible, which means that the molecule would lose energy due to collision and then recoils to a final state that is lower than the original energy state. In this case, the scattered photon will have frequency higher than the incidence frequency.

Figure (1.2) shows an inelastic scattering process between incident photon and a molecule causing transition to virtual state, then decaying to a final state different from the original one; in addition to emitting photon with frequency shift Δf.

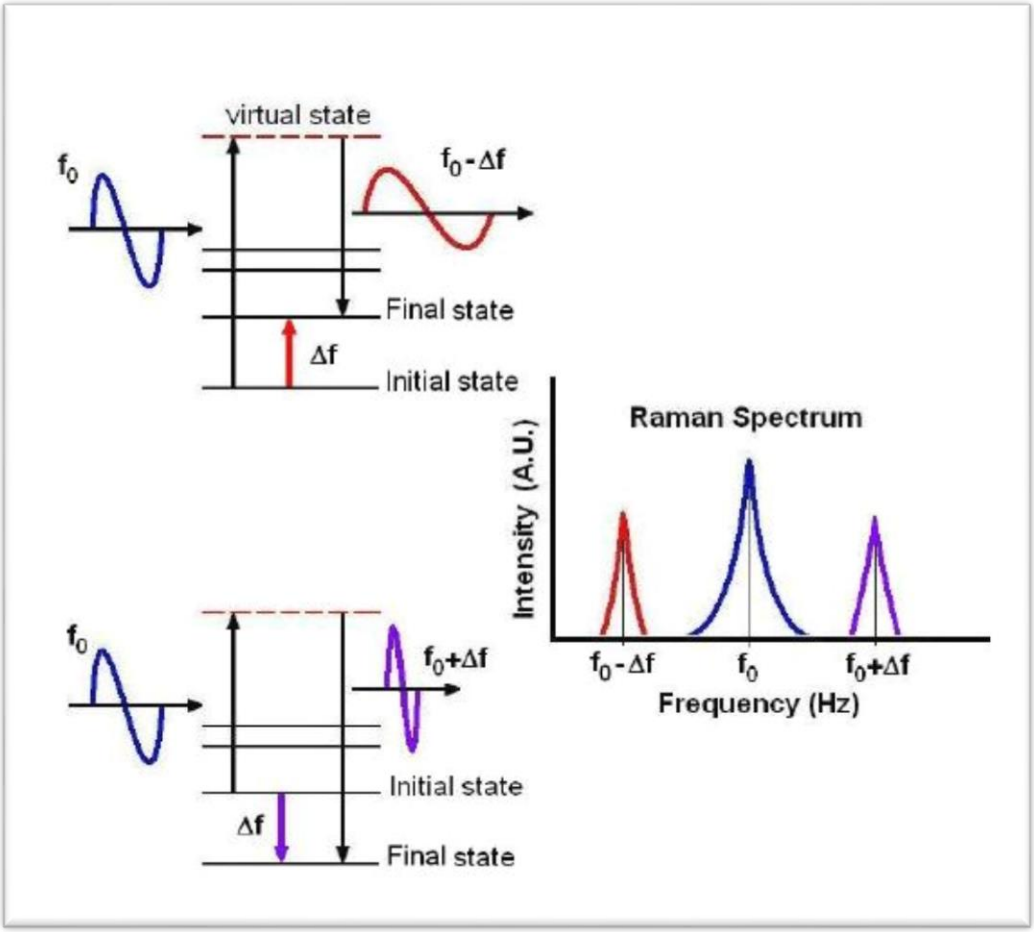

Figure 1.2: Raman inelastic scattering. From Zaghloul's thesis. [6]

1.3 Using Raman Spectroscopy to Investigate Clathrate Hydrates

Raman spectroscopy has proved a powerful tool to investigate clathrate hydrates during the past few years. Basically, Raman investigates the rotational and vibrational spectrum for molecules, so that we can know the rotational and vibrational behavior of the guest molecules. This means that we can develop a better and probably a full understanding about the enclathrated guest molecule's behavior inside cages.

Rotational spectra supply information concerning the motion of the guest molecules such as moments of inertia and inter-nuclear distances. Indeed, the rotational spectra are clear and easily interpreted. On the contrary, vibrational spectra consist of overlapping and contributions of different spectral lines in a way that makes it a little difficult to assign each peak to their corresponding vibrational excitation. Working out the whole spectral region of Raman Spectroscopy, especially the vibrational region, enables us to recognize the vibrational frequency, and then knowing the force constant which facilitate the process of modeling. In addition, an estimation of the number of molecules per cage can be given by interpreting the Raman spectrum.

1.4 Thesis Objectives and Outline

The aim of this research is to investigate binary clathrate hydrate of hydrogen and deuterium in sH structure using Raman spectroscopy. Accounting of previous research on clathrate hydrates will be introduced, and then the experiments that were conducted by our team will be discussed in details proposing solutions for some problems encountered in pervious literature.

In Chapter 2, Theory of Raman Spectroscopy will be discussed in more details according both classical and quantum explanations.

In Chapter 3, description and discussion of clathrates compounds, clathrate hydrates, hydrogen clathrates, and deuterium clathrates will be given.

In Chapter 4, previous work conducted on binary hydrogen and deuterium in different clathrate structures, especially sH and sII, will be referred.

In Chapter 5, Description of the experimental setup, procedure, and results will be presented in details. In addition, data analysis and discussion will be included showing assignment for vibrational peaks positions.

Chapter 2 : THEORY OF RAMAN SPECTROSCOPY

2.1 Classical Theory of Raman Effect

As the electromagnetic wave interacts with the molecule, the electric field (**E**) associated to the electromagnetic waves will polarize the charges of the molecule. As a result, an electric dipole moment (**P**) will be induced. The magnitude of the induced electric dipole moment is proportional to the magnitude of the electric field and is given by

$$P = \alpha E \ldots\ldots\ldots \quad (2.1)$$

Where α is the Polarizability of the molecule. The polarizability depends on the nuclear coordinates, which means that it is depending on molecular vibrational frequencies. So far, we aim to obtain the dependence of dipole moment on frequency, and for doing so we shall introduce the frequency dependence of (α) and (E) into equation (2.1). [5]

If the travelling electromagnetic wave has frequency *f*, the electric field is given by the following frequency dependence

$$E = E_0 \sin \omega t = E_0 \sin 2\pi f t \ldots\ldots\ldots\ldots \quad (2.2)$$

Where E_0 is the electric field intensity and t stands for time. As the electric field is time-dependent, the induced dipole moment will be time-dependent too. If the dipole moment is oscillating with the same frequency as that of the incident wave, it will also emit radiation with frequency equals to the incident beam, which means that the system undergoes Rayleigh scattering. However, if the polarizability varies somewhat with molecular vibration, the emitted frequency will be different from the incident frequency. So, we should take the frequency of molecular vibrations in our consideration. [5]

We can so define polarizability as

$$\alpha = \alpha_0 + \frac{d\alpha}{dq} q \ldots\ldots\ldots \quad (2.3)$$

Where α_0 is the polarizability at equilibrium configuration, and by equilibrium configuration we mean before incident light, and q is dimension coordinate describing the molecular vibrations. This coordinate can be rewritten as following

$$q = q_0 \sin 2\pi f_m t \ldots\ldots\ldots \quad (2.4)$$

Where q_0 is the molecular vibration amplitude and f_m is the frequency associated to the molecule, i.e. molecular frequency.

From (2.3) and (2.4):

$$\alpha = \alpha_0 + \alpha_1 \sin 2\pi f_m t \ldots\ldots\ldots \quad (2.4)$$

With

$$\alpha_1 = \frac{d\alpha}{dq} q_0$$

From (2.4), (2.2), (2.1), the dipole moment is given by

$$P = \alpha_0 E_0 \sin 2\pi f t + \alpha_1 E_0 \sin(2\pi f t) \sin(2\pi f_m t) \ldots\ldots\ldots \quad (2.5)$$

Given the following trigonometric relation

$$\sin x \ \sin y = \frac{1}{2}[\cos(x-y) - \cos(x+y)]$$

We can rewrite (2.5) as following

$$P = \alpha_0 E_0 \sin 2\pi f t + \frac{1}{2}\alpha_1 E_0[\cos 2\pi (f - f_m) t - \cos 2\pi (f + f_m) t] \quad (2.6)$$

So far we have got the relation that describes the dipole moment dependence on frequency. Equation (2.6) has three terms showing that the dipole moment has three frequency components which are:

i- f with amplitude $\alpha_0 E_0$

ii- $(f - f_m)$ with small amplitude $\frac{1}{2}\alpha_1 E_0$

iii- $(f + f_m)$ with small amplitude $\frac{1}{2}\alpha_1 E_0$

This means that the Raman spectrum basically contains one peak at the position of the incident frequency, and another two weak peaks such that $(f + f_m)$ is to the right from the basic peak and $(f - f_m)$ is to the left.

If the molecular vibration was not changing the polarizability, so $\frac{d\alpha}{dq} = 0$. This means that the dipole moment is oscillating with frequency equals to the incident frequency. It should be clear that the above formulation is correct for the molecular vibration and for the molecular rotation. From the above discussion, it is obvious that in order to have an active Raman spectroscopy, we should have $\frac{d\alpha}{dq}$ non zero for vibration or rotation.

So far, the classical theory correctly predicts the frequency dependence for Rayleigh scattering and vibrational Raman scattering. In addition, it shows that Rayleigh scattering depends on the equilibrium polarizability α_0, and that

vibrational Raman scattering depends on the derived polarizability α_1. As a result, classical theory is sufficient for the qualitative analysis that gives information about characteristics molecular vibrational frequencies. However, there are some limitations for classical theory as, for example, it cannot be applied on the molecular rotator. The experimental results show that Raman spectrum consists of specific lines for the molecular rotations; however, classical theory predicts a continuous frequency spectrum for the rigid rotator. This contradiction is due to applying the classical mechanics concepts to a microscopic system. Moreover, classical theory cannot provide information about how is the polarizability is connected to the microscopic properties of the scattering molecule. [5]

In conclusion, classical theory of Raman scattering can provide adequate information qualitatively agrees with the experimental results, however, for quantitative agreement, it is not sufficient. As a result, the quantum theory for Raman Spectroscopy is necessary for developing a correct quantitative explanation for the experimental result.

2.2 Quantum Theory of Raman Effect

The quantum theory introduces the concept that energy is quantized to discrete amounts of energy. Each quantum is known as photon has energy equals to hν.

For the Raman and Rayleigh scattering, when photons interacts with a certain molecule, they undergo different kind of scattering, either elastic scattering or inelastic scattering. If the collision was elastic, the incident beam will be scattered with the same incidence frequency giving what called Rayleigh scattering. However, if the collision was inelastic, the scattered photon's frequency will be shifted from the incident frequency. This means that photons might have lost or have gained some energy due to interaction with the targeted molecule. This amount of energy lost, or gained, corresponds to specific energy levels. [5]

Suppose that E_1 is the energy of incident photon, and E_2 is the energy of the scattered photon, and the energy difference them is given by

$$\Delta E = E_1 - E_2 \text{ .....} \quad (2.7)$$

Substituting for energy

$$\Delta E = h\nu_1 - h\nu_2 \text{.....} \quad (2.8)$$

Where h is Planck constant, $h\nu_1$ is the energy of incident photon. If the incident photon gained some energy upon collision, it will be scattered with frequency equals to $h\nu_1 + \Delta E$. However, if the photon lost some energy upon collision, it will scattered with frequency equals to $h\nu_1 - \Delta E$. This means that Raman spectra will include two different lines with frequencies equal to $\nu_1 + \Delta E / h$, and $\nu_1 - \Delta E / h$ to the right of the un-shifted line and to the left respectively, and these lines are indications for transitions to higher or lower energy states. It is useful to note that ΔE can take any arbitrary value according to the scattering molecule. [5]

As mentioned earlier in the introduction, in Raman spectroscopy when the molecule acquires some amount of energy, it would be excited to a higher virtual energy state, then it decay to a final vibrational, or rotational, energy state that is higher than the initial state. There are two possibilities of these transitions, which are Stokes Raman scattering and anti -Stokes Raman scattering. If the Raman spectral line appears at a lower frequency than the incidence one, it would be called Stokes line; however, if the Raman spectral line appears at a higher frequency, it would be called anti-Stokes line.

Figure (2.1) illustrates difference between Stokes and anti-Stokes transitions, in addition to some other kinds of scattering processes.

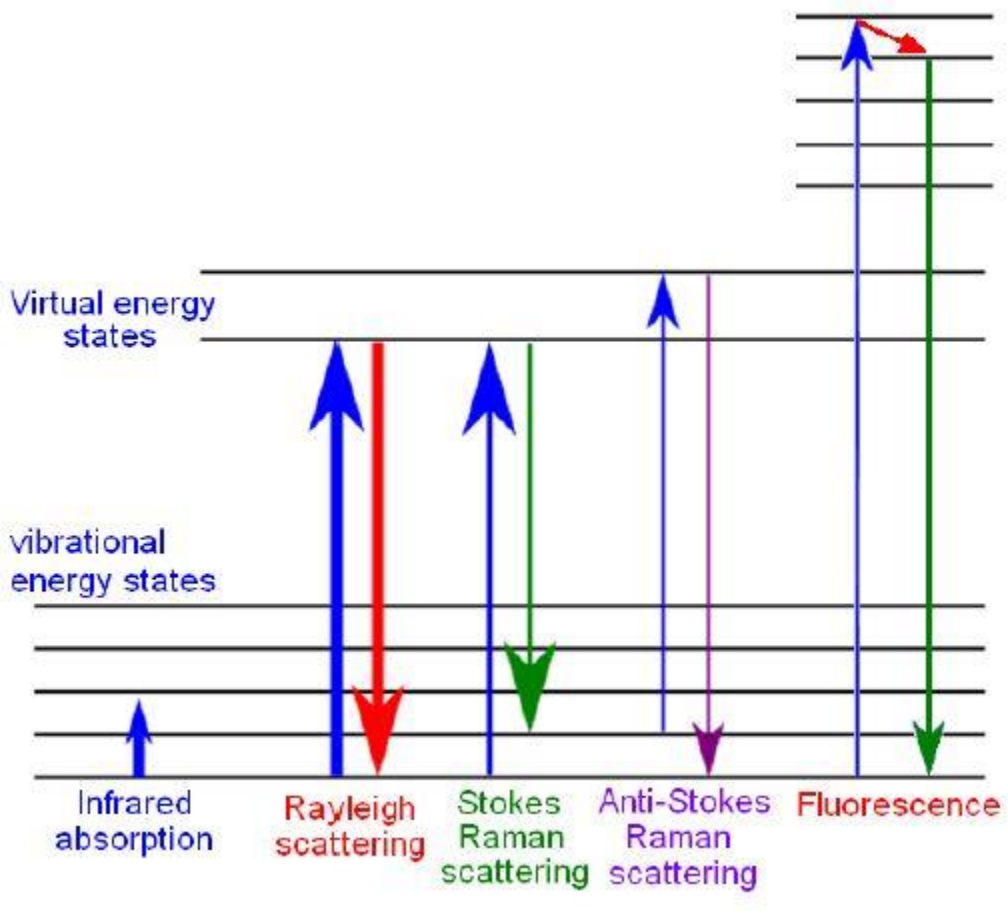

Figure 2.1: Different types of scattering processes. From Zaghloul's thesis. [6]

2.3 Quantum Agreement with the Classical Theory and Experimental results

In order to show that the quantum explanation for Raman scattering agrees with the classical theory and experiment date, let us use the wave notations. Consider that there is a transition occurs between two energy states n and m with wave functions ψ_n and ψ_m, so that the matrix element of the scattering moment is given by

$$[P]^{nm} = \int \psi_n^* P \psi_m dr \quad \ldots\ldots\ldots \quad (2.9)$$

For P under integration, we might substitute its value from equation (2.1). As the integrand ($\psi_n^* P \psi_m$) contains exponential depending on time, $[P]^{nm}$ will be a function of frequency and changes with $\nu_1 + (E_n - E_m) / h$. If we rewrite equation (2.9) regarding the amplitude, we would get the following

$$[P^0]^{nm} = \mathrm{E} \int \psi_n^* \alpha \psi_m dr \quad \ldots\ldots\ldots \quad (2.10)$$

The integrand of the above equation shows that, for two energy states E_n and E_m, transition from state n to state m is only possible in case that the integral is non-zero in presence of an electric field associated to the incident electromagnetic radiation with frequency ν_1. This transition appears in Raman spectrum at frequency $\nu_1 + (E_n - E_m) / h$, and is displaced form the incidence frequency by $(E_n - E_m) / h$. It is useful to note that the amplitude squared is proportional to the transition probability. This probability determines the intensity of Raman spectral line.

In addition, if the polarizability α in equation (2.10) was constant, so we can extract it out from the integral giving

$$[P^0]^{nm} = \mathrm{E}\alpha \int \psi_n^* \ \psi_m d \ldots\ldots\ldots \quad (2.11)$$

The above integral vanishes at all values except m = n because ψ_n^* and $\psi_m$are orthogonal. This means that for m = n we will get Rayleigh scattering as long as α is constant. However, Raman scattering will occur only if α is changing in case of rotations or vibrations. This explanation agrees with the classical theory in addition to the experimental results.

Chapter 3 : CLATHRATE COMPOUNDS, AND CLATHRATE HYDRATES

3.1 Clathrate compounds

Clathrate compounds are crystalline solid structures formed of two different molecules; one of them is called the host molecule which is forming the clathrate polyhedral cages with different size and geometry. The other molecule is the guest molecule which is trapped inside these cages. Clathrates are formed under certain values of pressures and temperatures. They physically look like ice, but with different internal structure. The term “Clathrate” is derived from the Latin word “Clathratus” which means closed inside bars. Actually, clathrate molecules are formed by a phase change process without any chemical reactions. However, the formation and composition details are still not fully understood.

3.2 Clathrate Hydrate

Clathrate have different types, and one of these types is the clathrate hydrate which is simply contains water as the host molecules. This water molecules, under low temperatures and high pressures, are the responsible of forming cages in which different guest molecules, such as hydrogen, deuterium, CH_4…etc, would be trapped. Such cages are with size approximately equals to 1 nm. The guest molecule is highly significant concerning clathrate stability, this is because the absence of guest molecule means that the clathrate as whole will collapse into conventional ice or simply liquid water.

Scientists usually classify clathrate hydrates according to their crystalline structures. Structure I (sI), and Structure II (sII), and the hexagonal structure (sH) are the three possible types for clathrate hydrate crystalline structure. The difference between each one of them is based on the cage size and geometry which represents the amount of water molecules required to produce a molecular cage. In order to recognize the geometry of cavities, we use the following nomenclature

$$A^x B^y \ldots\ldots\ldots \quad (3.1)$$

Where x is the number of faces with molecule A per cage, and y is the number of faces with molecule B per cage. For example 5^{12} mean that the cage has 12 faces of pentagons. The most common crystal structures sI, sII, and sH are shown in figures (3.1), (3.2), (3.3) respectively.

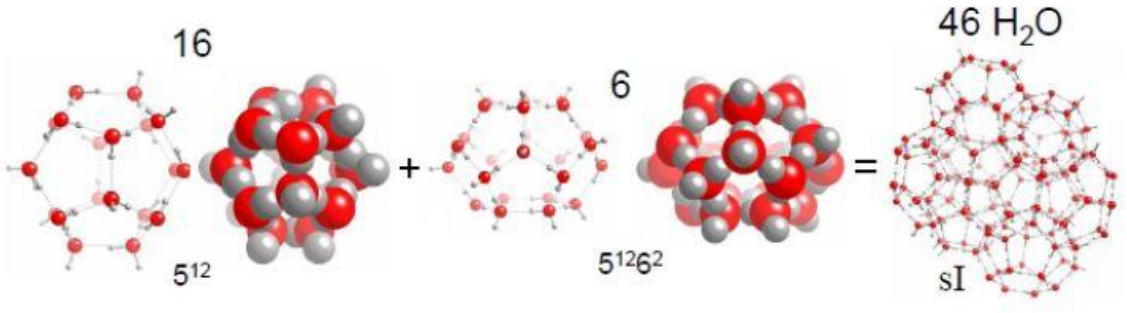

Figure 3.1: Sixteen small cages (5^{12}) and 6 large cages ($5^{12}6^2$) forming a unit cell of sI crystalline structure which contains 46 molecules of water. From Zaghloul's thesis, and Strobel's thesis. [6][7]

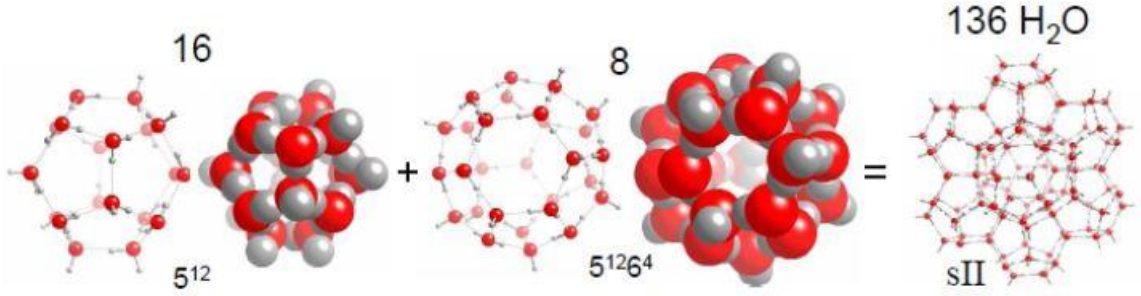

Figure 3.2: Sixteen small cages (5^{12}) and 8 large cages ($5^{12}6^4$) forming a unit cell of sII crystalline structure which contains 136 molecules of water. From Zaghloul's thesis, and Strobel's thesis.[6][7]

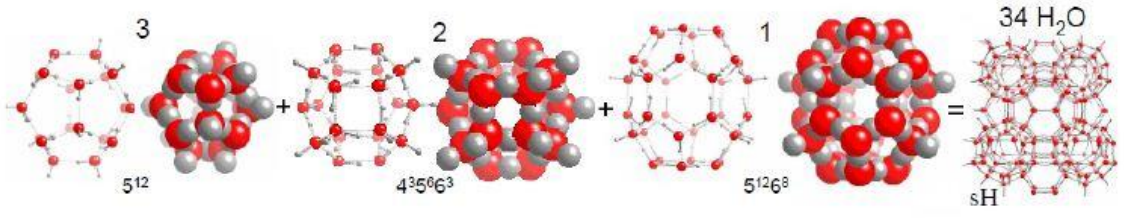

Figure 3.3:Three small cages (5^{12}) and addition two middle cages ($4^35^66^3$) and one large cage ($5^{12}6^8$) forming a unit cell of sH crystalline structure which contains 34 molecules of water. From Zaghloul's thesis, and Strobel's thesis. [6][7]

Actually, the existence of these three crystalline structures are considered to be a function of the guest molecule's size

First of all, crystal structure sI is the smallest possible crystal for clathrates. It is a type of the space group *Pm3n* with lattice spacing (a ~ 12 Å). Clathrates with this structure can trap molecules with size ranging from (d ~ 4-6 Å), for example methane CH_4 and ethane C_2H_6 and carbon dioxide CO_2. This structure forms a unit cell with sixteen small cages (5^{12}) in addition to another six large cages ($5^{12}6^2$) with 46 molecules of water as shown in figure (3.1). This classification of small and large cages means that this structure has twelve polygonal faces of water molecules belonging to the small cage in addition to another twelve polygonal faces of water molecules belonging to the large cage. Moreover, two polygonal face of six molecules of water.

The second possible structure is sII. Crystal structure sII is a type of the space group $Fd\bar{3}m$ with lattice spacing (a ~17 Å). Clathrates obeying this type of crystal structure usually have guest molecules with size ranging from (d ~ 4-6Å) such as C_3H_8, and small formers (d ~ 4 Å) such as N_2. This combination forms sII unit cell with sixteen small cages (5^{12}) in addition to eight large cages ($5^{12}6^2$) with 136 molecules of water. These details are shown in figure (3.2).

Last but not least, crystal structure sH is the clathrate structure that can trap the largest molecules because it possesses the largest cage among all other clathrate crystal structures. Crystal structure sH is a type of the space group *P6/mmm* with lattice spacing (a ~ 12, c~10 Å). The unit cell of this hexagonal sH lattice consists of three small cages (5^{12}) with two small cages ($4^3 5^6 6^3$) in addition to one large cage ($5^{12}6^8$), along with 34 molecules of water as shown in figure (3.3). As this hexagonal lattice is the largest, it is able to trap guest molecules with (d~7.5-9 Å). In order to achieve structure stability, the large cage should be occupied by a large

molecule such as THF (tetrahydrofuran) or MTBE (methyl tertiary butyl ether) for structure stability reasons, while the small and medium cages might be occupied by smaller molecules such as methane, hydrogen or deuterium.

Figure (3.4) shows a comparison between different molecules with respect to diameter, referring size, and their corresponding crystal structure.

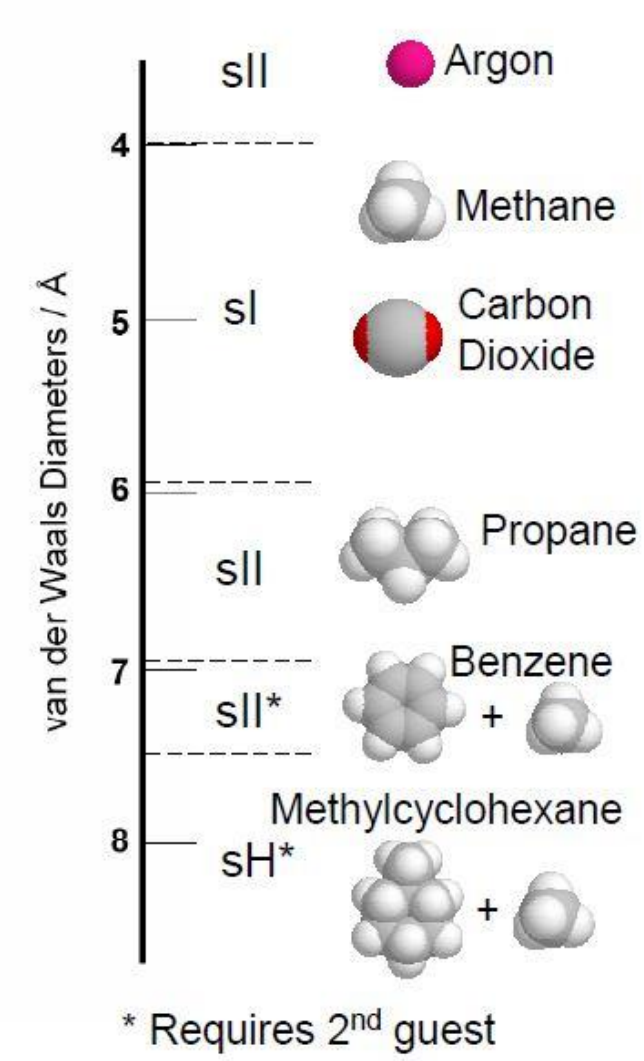

Figure 3.4: Different guest molecule with respect to size and their corresponding possible crystal structure. From Strobel's thesis. [7]

3.3 Hydrogen Clathrate Hydrate

If the trapped guest molecule was hydrogen or deuterium, the formed clathrate hydrate would be called hydrogen clathrate hydrate. It is known that conventional methods of storing hydrogen are usually dangerous and expensive because hydrogen is one of the most explosive materials, so that requiring extreme conditions for storing. However, hydrogen clathrate hydrate is promising as a safe and economic method to store hydrogen. This means that hydrogen clathrate hydrate can be considered as fuel storage.

Commonly, hydrogen is enclathrated with water into crystal structure sII. As mentioned above, this kind of crystal structure has a cubic structure containing 136 molecules of water forming one unit cell. This unit cell contains sixteen small cages, and eight large cages. The small cage is dodecahedron with twelve pentagonal faces with abbreviation of 5^{12}, while the large cage is hexakaidecahedron with twelve pentagonal and another four hexagonal faces with abbreviation of $5^{12}6^{4}$. [8]

Historically, it was thought that hydrogen cannot be used as a guest molecule that is stabilizing the clathrate hydrate compound because of its small size. [9] Nevertheless, during the last few years of experiments it was shown that hydrogen can be used to stabilize the clathrate compound either if it was the only guest molecule or along with other molecules. There are two types of hydrogen clathrates, which are simple and binary hydrogen clathrate. The simple hydrogen clathrate means that the hydrogen molecule is the only guest molecule to be exist in the clathrate compound. However, binary clathrate means that there is another guest molecule, for example MTBE, along with hydrogen and occupying the large cage. [8]

Scientists believe that either for simple or binary clathrate, the small cage is occupied by only one molecule of hydrogen; however, for the large cage it differs from simple to binary clathrate. For the simple clathrate, the large cage might be occupied by maximum of four molecules of hydrogen. On the other hand, the large cage of binary clathrate is occupied by one large molecule such as THF, tetrahydrofuran.

Nevertheless, other crystalline structures, sH and sI, can be formed also in case of hydrogen, but with special conditions and circumstances that gives binary clathrate. For example, in order to get sH structure with hydrogen, a large molecule such as MTBE should be introduced to occupy the large cage for stability reasons. [14]

In other context, it is useful to discuss the rotation behavior as it implies interesting information about hydrogen properties. Hydrogen and deuterium, hydrogen isotope, existing in gaseous state, are behaving as a quantum rotator with the following rotational energy

$$E(J) = B_0 J[J+1] \ldots\ldots\ldots\ldots \quad (3.2)$$

Where J is the rotation quantum number, B_0 is the rotational constant. In case of rotational ground state, the value of this constant for hydrogen is approximately about 59.322 cm^{-1} and for deuterium is about 29.904 cm^{-1}. [10] In case of diatomic molecules of similar atoms such as H_2, there are two isomeric forms depending on the nuclear spin.

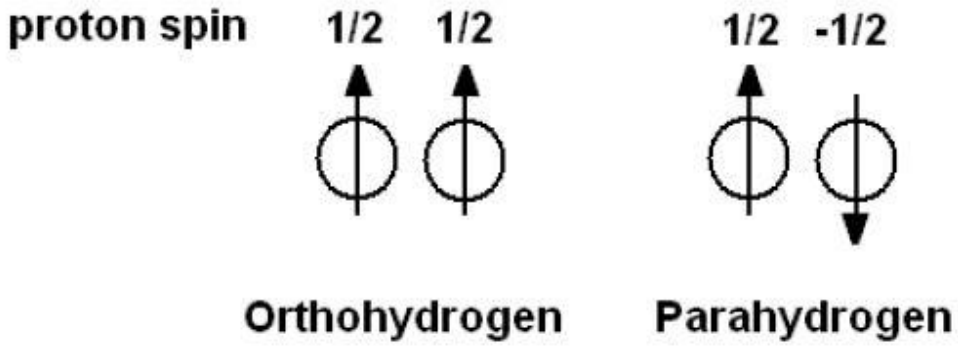

Figure 3.5: : Ortho and parahydrogen with their parallel and anti-parallel nuclear spins. From Zaghloul's thesis. [6]

For H_2 nuclei that obtain two indistinguishable fermions, there is a constraint that the total wave function should be anti-symmetric in case of nuclear exchange. So far there are two types of hydrogen [8], which are going to be defined below. First one is called parahydrogen defined as the case at which H_2 possess anti-parallel nuclear spins, spins are $^1/_2$ and – $^1/_2$. As a result of this spins, Parahydrogen has a zero molecular spin quantum number (I). In addition, parahydrogen has only even rotational states *J = 0, 2… etc.* On the other hand, hydrogen with parallel spins $^1/_2$ and $^1/_2$ is called orthohydrogen with molecular spin quantum number *I = 1*, and exist with odd rotational states J = 1, 3… etc. Figure (3.5) shows the two types of hydrogen.

Indeed, both orthohydrogen and parahydrogen exist at the same time with some specific concentration depending on temperature and other factors.
As the temperature is given by

$$T \gg \frac{B_0 hc}{k_B} \ldots\ldots\ldots \quad (3.3)$$

Where c is the speed of light in vacuum, and k_B is the Boltzmann constant, and h is plank constant. In fact, this temperature dependence comes up from the rotational energy dependence on temperature. At relatively high temperatures, both the free H_2 gas and enclathrated H_2 molecules obey a certain ratio of ortho to parahydrogen. The ortho to para ratio $\frac{n^o}{n^p}$ for hydrogen can be given by the following equation

$$\frac{n^o}{n^p} = 3\ \frac{\sum_{J=odd}(2J+1)\exp(-\beta E(J))}{\sum_{J=even}(2J+1)\exp(-\beta E(J))} \ldots\ldots\ldots \quad (3.4)$$

With

$$\beta = \frac{1}{k_B T}$$

Where (2J+1) stands for the rotational energy level degeneracy, and the factor of 3 come from the ratio of statistical weight. This means that the ratio of ortho to parahydrogen is 3:1. In addition, concentration equilibrium between them exists always for every temperature, and if the equilibrium was not satisfied within a given system at a certain temperature, the system tends to reach equilibrium through ortho-para conversion. [7]

Figure (3.6) shows the conversion process between ortho para as a function of temperature, in addition to a comparison between hydrogen and deuterium in terms of the conversion process. It is clear that the ration differs from hydrogen to deuterium provided that the process is reversed from one gas to another. The distribution shown in figure (3.6) has been calculated using equation (3.4).

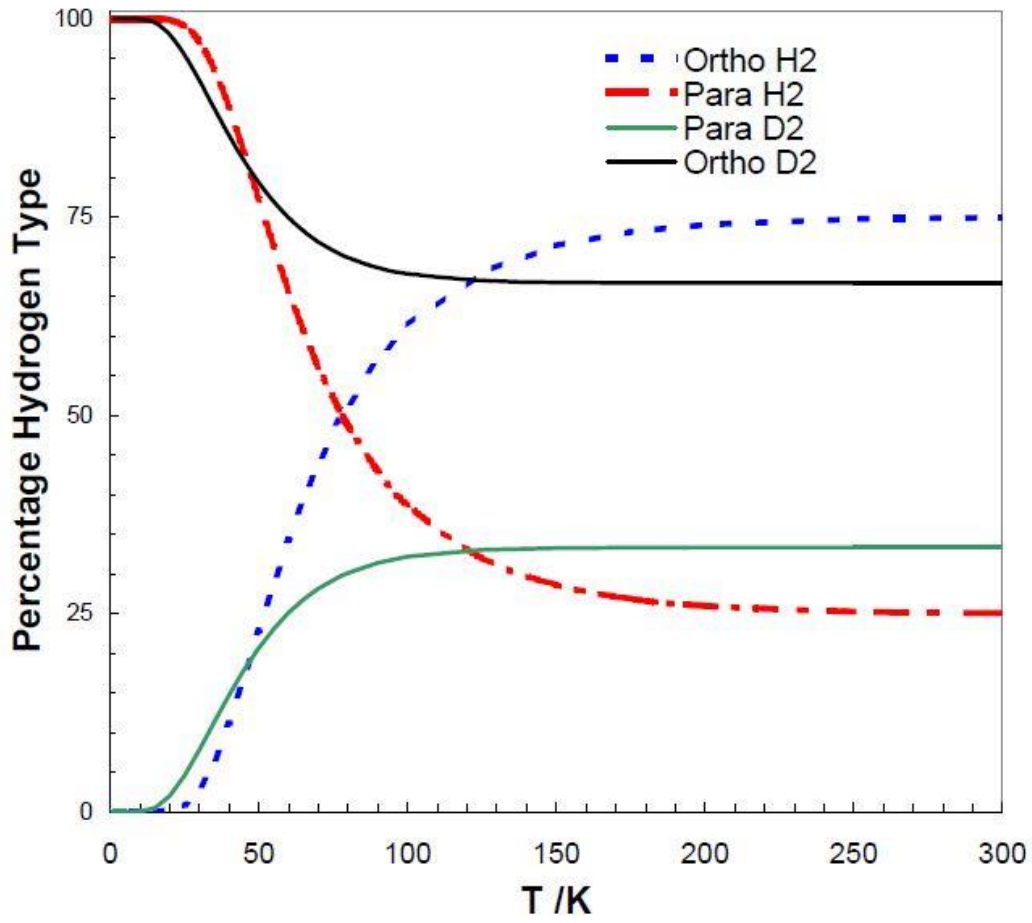

Figure 3.6: Ortho and para for hydrogen and deuterium as a function of temperature. From Strobel's thesis. [7]

At extremely low temperatures, around absolute zero, the concentration is almost 100% parahydrogen, so that parahydrogen is dominant at low temperatures, and it is more likely to encounter conversion from ortho to para at these low temperatures. However, conversion from para to ortho also exists and will be discussed later on.

Deuterium is generally like hydrogen, with some differences in details, it has the two types ortho and para. The nuclei of D_2 consist of two indistinguishable bosons with constraint on the total wave function to be symmetric in case of nuclear exchange. So that, orthodeuterium consists of those molecules with molecular spin quantum number $I = 0, 2$ with even values of rotational states $J = 0, 2$….etc. In addition, Paradeuterium composed of those molecules with $I = 1$ and odd values of rotational states J = 1, 3…etc. Unlike hydrogen, deuterium has ortho to para concentration ratio of 2:1 according to statistical weight.

3.4 Formation and Decomposition of Hydrogen Clathrate Hydrate

It was accounted into the above introductory sections that the nature of clathrate formation and decomposition is not yet fully understood, however, the formation and decomposition conditions are known as a result of several experiments performed on clathrates. In order to form a clathrate hydrate, water is required in addition to a plenty of gas, and both would, favorably, be admitted to environment of low temperature and high pressure. However, some clathrates are found to be formed at temperatures higher than 300 K and near to the atmospheric pressure, but this depends on the gas that is forming clathrate. [9]

In case of the simple clathrate, scientists found that hydrogen clathrate hydrate can be formed at pressures around 2000 bar at temperature of 273 K. If pressure decreased, temperature should also be decreased in order to get a phase transition to the clathrate. It is possible to increase the population of guest molecules by two actions, one of them is increasing the applied pressure, and the other is decreasing the temperature. Although, both actions lead to the same result finally, decreasing temperature is slowing down the formation process as the energy of molecules decreases by decreasing temperature.

On the other hand, decomposition happens if the formation factors were reversed, which means that increasing temperature would simply decrease the population of guest molecules gradually until the whole system eventually collapse to conventional ice or even water. Also, decreasing pressure to few bars would perform similar to decreasing temperature.

Figure (3.7) is a phase diagram showing the required pressure and temperature to get clathrate hydrate compound formed, while figure (3.8) is a phase diagram shows a comparison between clathrate formations with different guest molecules of rare gases.

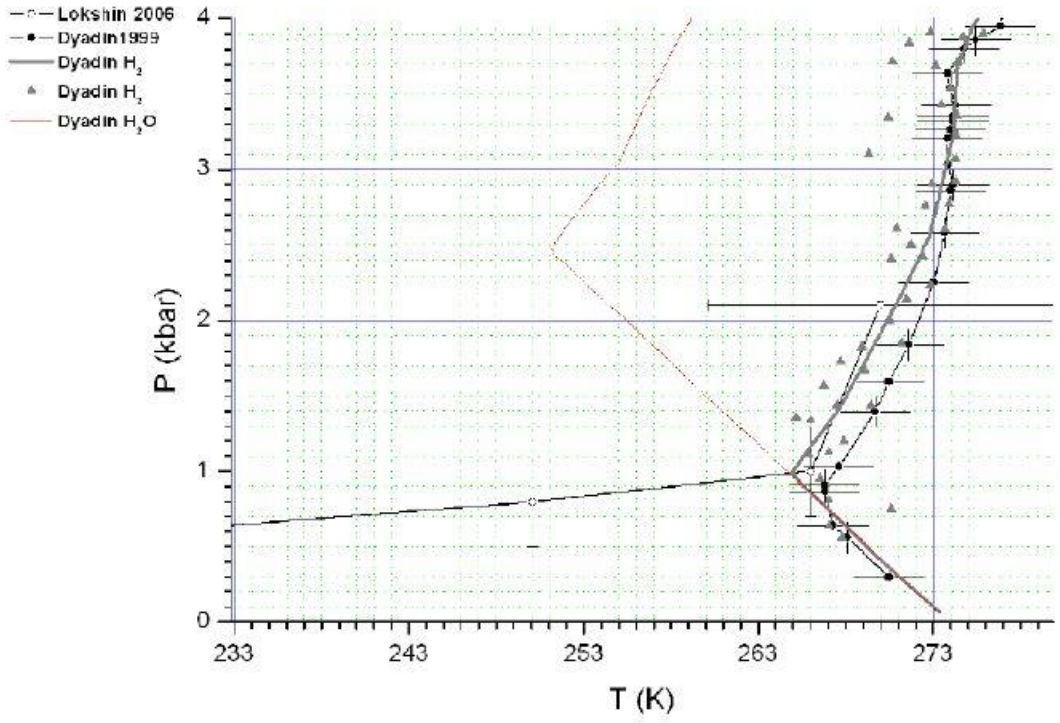

Figure 3.7: Phase diagram of hydrogen clathrate hydrate formation introduced by Dyadin[11], Lokshin[12], and Duarte. [13] [6]

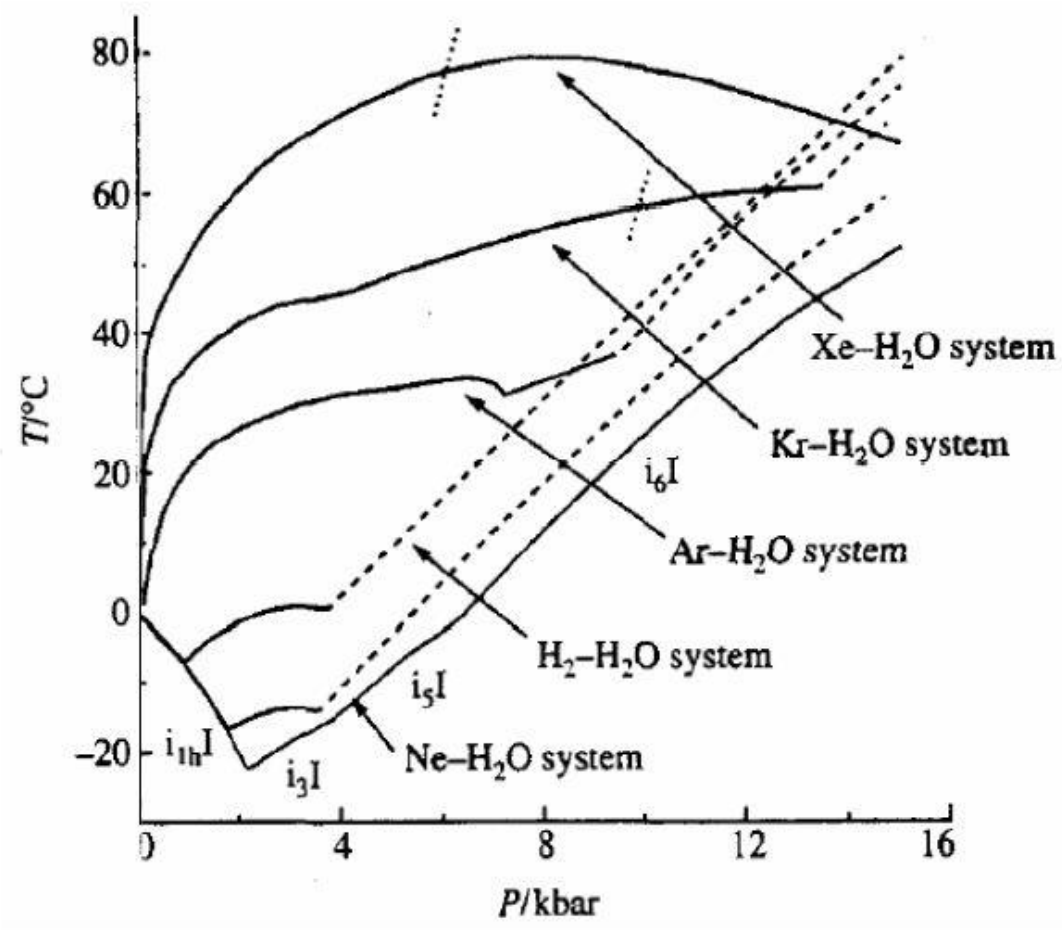

Figure 3.8: Phase diagram for hydrogen clathrate hydrate and other clathrates with rare gases. [7] [13]

Chapter 4 : INVESTIGATING HYDROGEN CLATHRATE HYDRATES USING RAMAN SPECTROSCOPY

4.1 Introduction

As mentioned earlier, there are different methods to study clathrate hydrate behavior such as neutron scattering, NMR (Nuclear Magnetic resonance), Infrared, and Raman spectroscopy. However, in this research we are using Raman spectroscopy to investigate clathrates, and particularly the vibrational and rotational behavior of the guest molecules inside the clathrate polygon cage.

Estimating the excitation modes and vibrational or rotational transitions is possible by investigative the Raman spectrum. Next, a discussion of recent research conducted to explore clathrate hydrates using Raman spectroscopy would be introduced. It might be useful to know about the behavior of guest molecules in case of simple clathrate in order to compare it with their behavior in case of binary clathrate. In addition, knowing the cage occupancy for the sII structure enables us to correctly predict the occupancy for sH cages by comparing frequencies.

4.2 Analysis of rotational modes using Raman spectroscopy

In case of Raman spectrum, the pure rotational excitations have frequencies given by $S_0\ (J)$, with ΔJ indicates the transition that is $\Delta J = J \rightarrow J'$ (J' is the final state). Quantum mechanically, rotational transitions are possible only at a

certain values and are forbidden elsewhere. Consequently, the selection rule for rotational transitions in case of Raman scattering is given by $\Delta J = 0, \pm 2$ with a wave function constraint that is not allowing transition ± 1.

The rotational spectrum of H_2 and D_2 gas at room temperature is given by Figure (4.1). At room temperature, the rotational Raman spectroscopy for hydrogen gas H_2 shows four spectral lines, S_0 (0), S_0 (1), S_0 (2), S_0 (3), which are equally spaced clarifying the populated rotational energy levels. On the other hand, rotational Raman spectroscopy for deuterium gas D_2 at room temperature shows five spectral lines. This increase in the number of spectral lines is due to the increased mass of deuterium from hydrogen, which leads to a small increase in the rotational constant. Moreover, comparison between H_2 and D_2 shows that the spectral lines for deuterium are shifted to the lower frequency by factor of two because of the mass difference.

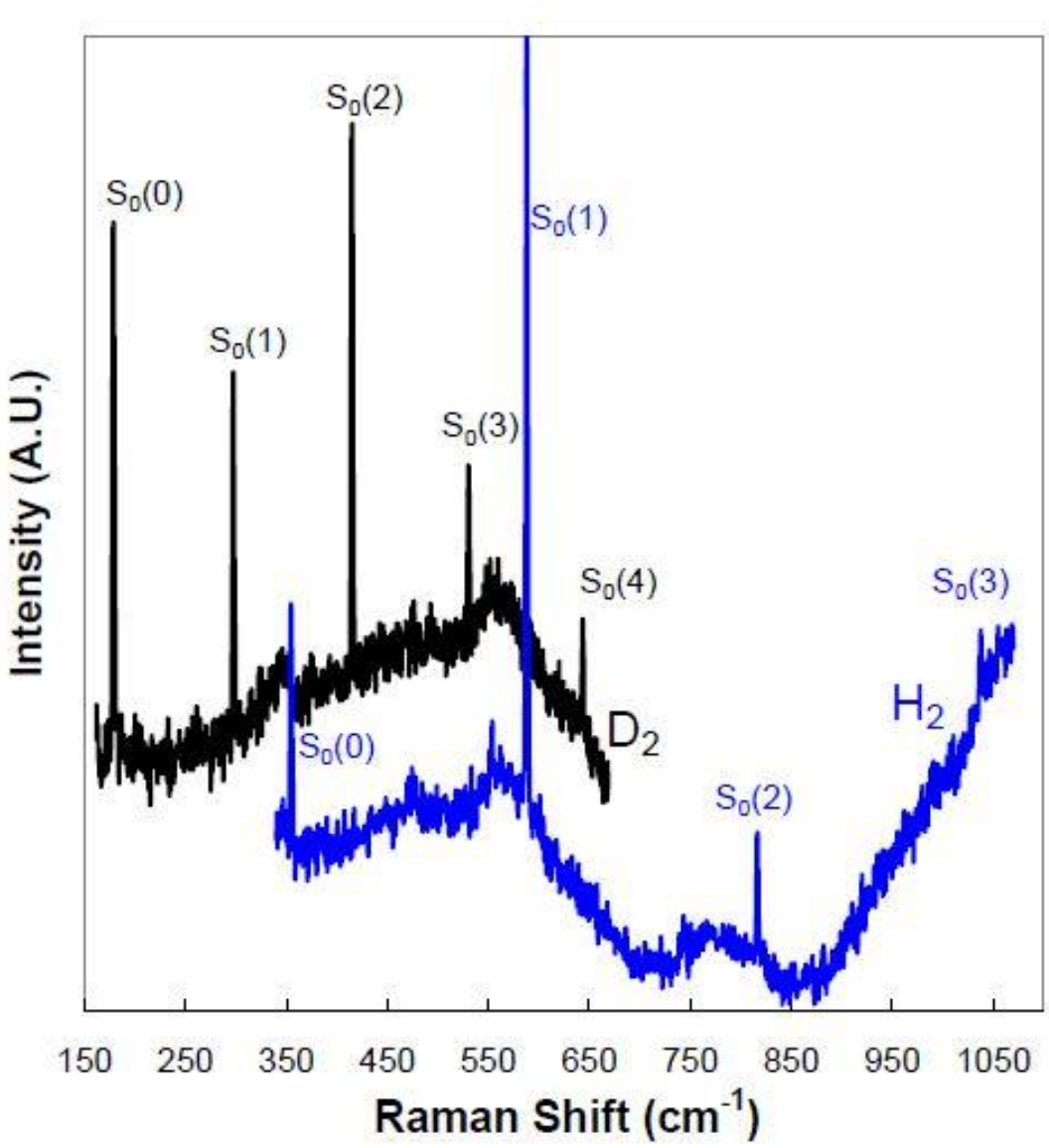

Figure 4.1: Raman spectrum for rotational transitions for H2 gas (blue line/ at bottom) and D2 gas (black line / top) at room temperature at pressure of 1 bar. From Strobel's thesis. [7]

As the temperature decreases approaching the boiling point of liquid nitrogen, it would be harder to observe the higher frequency spectral lines, and only the two observable spectral lines are S_0 (0), S_0 (1). This is because at lower temperatures, the higher energy rotational bands became un-populated. Spectral line S_0 (0) represents the rotational transition $\Delta\upsilon = 0$ with $J = 0 \rightarrow 2$ of parahydrogen,

and the spectral line S_0 (1) represents the orthohydrogen rotational transition $\Delta\upsilon = 0$ with $J = 1 \rightarrow 3$. As the clathrate formation occurs, spectral lines S_0 (0), S_0 (1) are observed to be shifted from their original positions in case of free gaseous state with more broadening. For simple hydrogen clathrate, S_0 (0) appears at 350 cm^{-1} approximately, while S_0 (1) appears at about 580 cm^{-1}. Comparing the spectral lines of S_0 (0) for clathrate hydrogen and free gaseous hydrogen and the same for S_0 (1) shows that the frequencies are quite close, which means that enclathrated H_2 molecules are almost rotating freely.

In case of having a diatomic molecule consists of two identical atoms, such as H_2, the rotational energy states would be degenerated by 2J+1, such that the third quantum number m takes values of J, J-1, …, -J+1, -J.

In case of J=0, the only possible value for m is to be zero, and then the spherical harmonics probability density would be given by sphere which is isotropic (i.e. with no orientation dependence). While if J =1, n would take either zero or 1 or -1, and the spherical harmonics probability would then be given by spheroids, which are flattened or elongated. Indeed, m values for free hydrogen molecules would be degenerated, means that m energy levels would have the same energy, so that rotational population factor will only be affected, which in turn affect the Raman peaks intensities. [8]

Figure (4.2) illustrates the degenerated rotational energy levels in case of free hydrogen molecules.

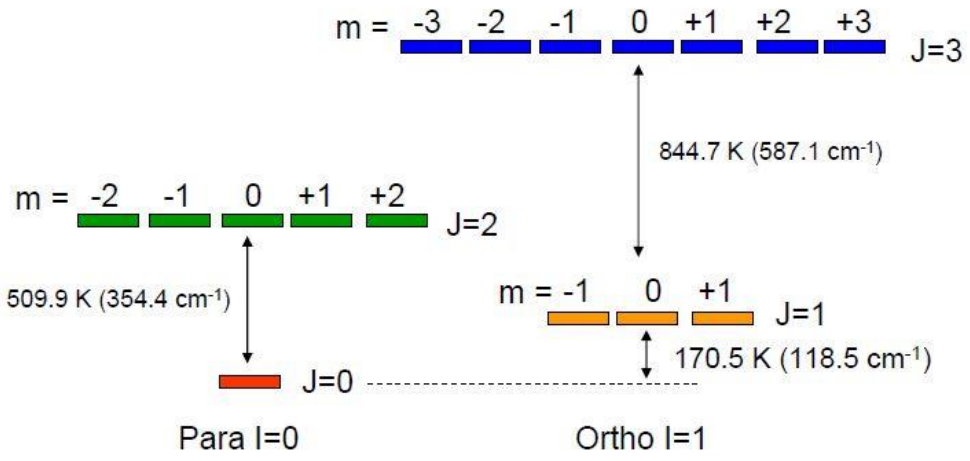

Figure 4.2: Rotational energy levels. From Strobel's thesis. [7]

In the case of parahydrogen, there would be five different possibilities for the transition J = 0→ 2 as the hydrogen molecule may undertake transition from the level of J = 0, m = 0 to any of the five m levels of J= 2. This means that it is expected to have five noticeable peaks for parahydrogen. However, there were only three peaks reported by Giannasi for the rotational parahydrogen as shown in figure (4.3)

For the H_2 molecule occupying the small cage, it was found that the five energy levels, which are associated to J = 2 level, appear at 348.6, 349.6, 356, 363.4, and 364.3 cm^{-1}. Apparently, the first two values are so much close to each other as well as the last two values, which means that roughly there are three noticeable spectral lines in agreement with the spectral line splitting shown in Figure (4.3)

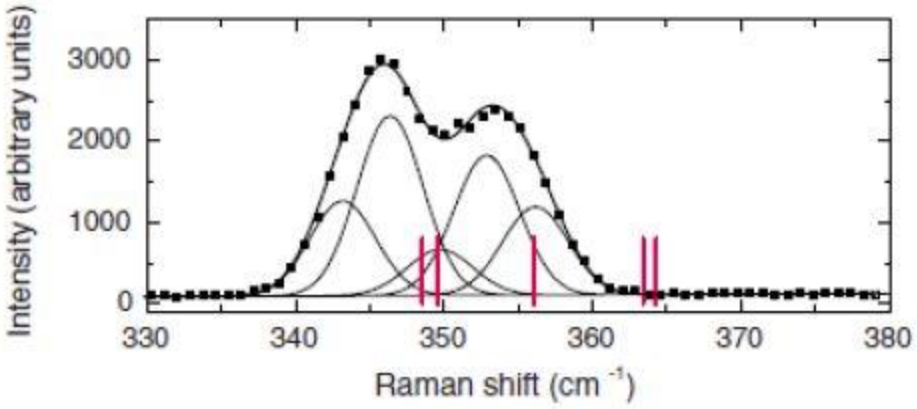

Figure 4.3: S0 (0) Rotational peak for parahydrogen. From Giannasi et al (2008).

In the case of orthohydrogen, because there are lots of transition possibilities from the three different m sublevels associated to J = 1 and the seven different m sublevels associated to J = 3, there is no obvious spectral line splitting can be observed.

Indeed, the rotational Raman spectra show that there is a superposition contribution from both orthohydrogen and parahydrogen for small and large cages in case of the simple sII clathrate hydrate. As a result of that, Giannasi analyzed these peaks at 2011in order to reveal the exact contribution of each cage. This analysis suggested that the small cages for both simple and binary clathrate to be the same with approximately identical molecular behavior inside the small them. Moreover, Giannasi claimed that each small cage is occupied by only one hydrogen molecule. The last finding was introduced when an experiment carried out with pressure of 800 bars applied to form a binary clathrate with support of THF with low temperature down to 20K. Thus, the resulting peaks of S_0 (0) and S_0 (1) were representing the contribution of hydrogen from small cage only. However, the early presented peaks for simple clathrate were representing hydrogen contribution from both small and large cages. Finally, Giannasi

subtracted the date representing binary clathrate from data representing simple clathrate in order to get hydrogen contribution from large cage only as shown in figure (4.4)

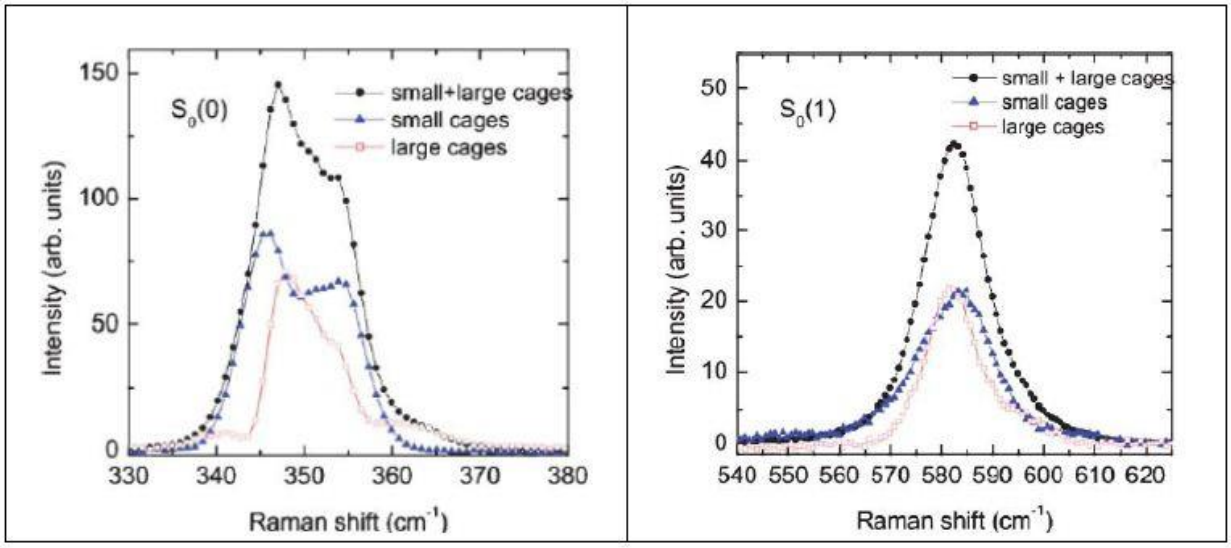

Figure 4.4: Parahydrogen S0 (0) and orthohydrogen one by one with precious assignment for small and large cage contributions .From Giannasi et al (2011).

In addition, Giannasi estimated the hydrogen population in each cage, either small or large cage, by analyzing the intensity of different peaks, which represent different cage contribution. According to Giannasi, around 60% of the total amount of hydrogen molecules occupies the small cages, whereas the large cages are approximately occupied by the remaining 40% of the hydrogen molecules. Given that the number of small cages is approximately twice the number of large cages, Giannasi suggested that the average occupancy, which refers to the number of molecules per cage, for large cage is 1.33 for the sample used in such experiment. Additional verification for such result has been carried out by investigating the vibrational spectrum.

4.2.1 Ortho Para Conversion

As shown above at chapter three, in a sample of free hydrogen gas, orthohydrogen is dominant at high temperatures providing that the ratio of orthohydrogen to parahydrogen is 3:1. While for deuterium, the ratio of orthodeuterium to Paradeuterium at high temperatures is 2:1, knowing that these ratios are due to statistical weight. As the temperature decreases during the formation of clathrate, orthohydrogen converts to parahydrogen gradually, and eventually the sample would be dominated by parahydrogen. Indeed, this conversion process occurs because of an intrinsic reason in addition to another external one. The external reason is the existence of a microscopic magnetic field, which acts a catalyst, while the intrinsic one is related to temperature. Knowing that the time required for conversion process differs for intrinsic reason from extrinsic one, the conversion for trapped molecules inside cages would be slower than the free molecules. This is because there is no external catalyst acting on the trapped molecules.

In the same context, Giannasi[22] mentioned that it is possible to calculate the population of parahydrogen $X_p$using the intensities of rotational Raman spectral lines S_0 (0), S_0 (1). This can be done using the following equation

$$\frac{I_{s_0}}{I_{s_1}} = \frac{b_{02}}{b_{13}} \frac{\gamma_0^2}{\gamma_1^2} \frac{\upsilon_0^3}{\upsilon_1^3} \frac{X_p}{1-X_p} \frac{P_0}{P_1} \ldots\ldots\ldots \quad (4.1)$$

Where

I_{s_0}: The area under S_0 (0), while I_{s_1}stands for the area under S_0 (1)

b_{02}: The statistical weight for transition from 0 to 2, and the same forb_{13}.

γ_i : The polarization anisotropy for the initial energy state

υ : the frequency of the scattered radiation

P_0 : The parahydrogen population at energy state $J = 1$

P_1 : The orthohydrogen population at energy state $J = 2$

4.3 Analysis of Vibrational modes using Raman spectroscopy

The Raman spectrum at room temperature for hydrogen molecules at gaseous state shows four spectral peaks representing transitions in the Q branch. [14] The frequencies of vibrational transitions are given by $Q_{\Delta\upsilon}(J)$, where υ is the vibrational quantum number, while J is the rotational quantum number, and $\Delta\upsilon = \upsilon \rightarrow \upsilon'$ (which will be 1 in this research). The observable four spectral are $Q_1(3)$, $Q_1(2)$, $Q_1(1)$, and $Q_1(0)$; where the intensity of the second peak $Q_1(1)$ will be dominated by the ortho-para ratio and by the rotational population rotational factor. [14] Figure (4.5) shows a comparison between Raman spectrum obtained from gaseous hydrogen and gaseous deuterium at room temperature and pressure equals to 1 bar. It is obvious that the number of peaks for both hydrogen and deuterium is the same like the rotational spectra. It is noticeable that deuterium spectral lines are shifted to a frequency lower than the hydrogen frequency.

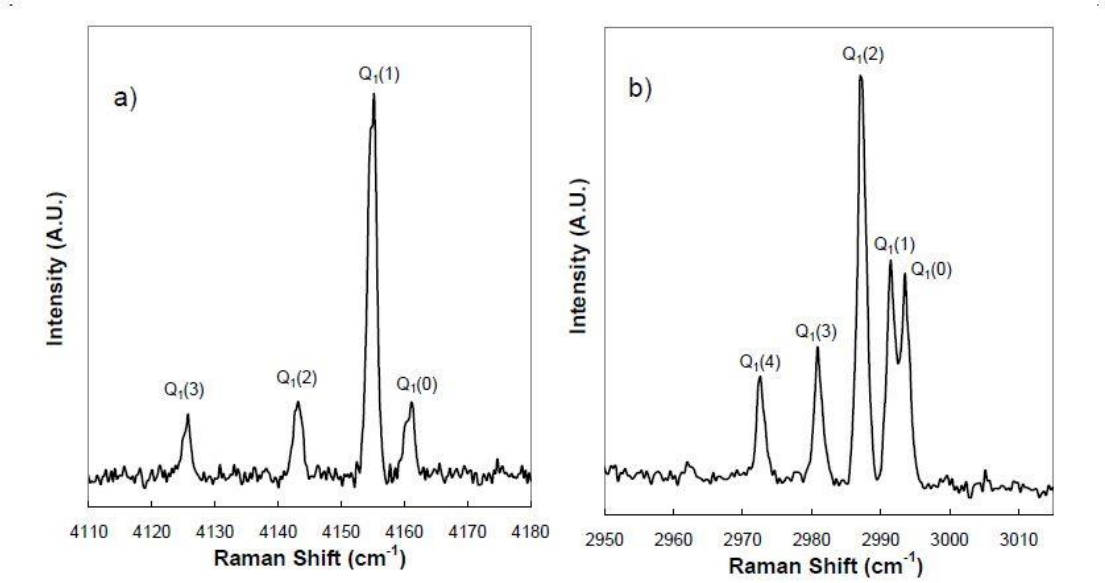

Figure 4.5: Vibrational Raman spectrum form H_2 (left) and D_2 (right) at room temperature and pressure of 1 bar. From Strobel's thesis. [7]

The intensities of these vibrational bands depend on the population of rotational energy levels, and on the nuclear spins. [7]

Decreasing the temperature down to the boiling point of liquid nitrogen, the highest rotational energy levels would not be populated, which means that the intensities of the corresponding vibrational bands will fall down. As a result of that, the only observable peaks will be Q_1 (1) approximately at 4155 cm^{-1} and Q_1 (0) approximately at 4161 cm^{-1}. For investigating clathrate hydrate for hydrogen, Strobel carried out experiments at which he got Raman spectrum for sH structure binary hydrogen clathrate hydrate, in addition to Raman spectrum for sII binary tetrahydrofuran (THF) / H_2 clathrate hydrate. Then, he compared between spectrum obtained from sH structure and spectrum obtained from the well-known sII structure and spectrum obtained from the pure hydrogen gas. Figure (4.6) shows the vibrational Raman spectrum for pure H_2 gas, and binary sII hydrogen clathrate with THF, and binary sH hydrogen clathrate with MTBE (methyl tert-butyl ether) and with MCH (methylcyclohexane) and with 2, 2, 3-TMB (trimethylbutane).

For the THF/H_2 sII clathrate, lots of studies have already shown that THF occupies the large cage, while the small cage is occupied by only one hydrogen molecule; which is applied under pressures up to 3500 bar.[15]-[19] As a result of that, Stobel assigned vibrational spectral peaks, in figure (4.6) that appears at 4119 and 4124 cm^{-1} to the transitions Q_1 (1) and Q_1 (0) respectively.[14] Indeed, this assignment has been reinforced by the fact that the separation between Q_1 (1) and Q_1 (0) is approximately 5 cm^{-1}, which is comparable to the 6 cm^{-1} separation between Q_1-(1) and Q_1 (0) in gaseous state.

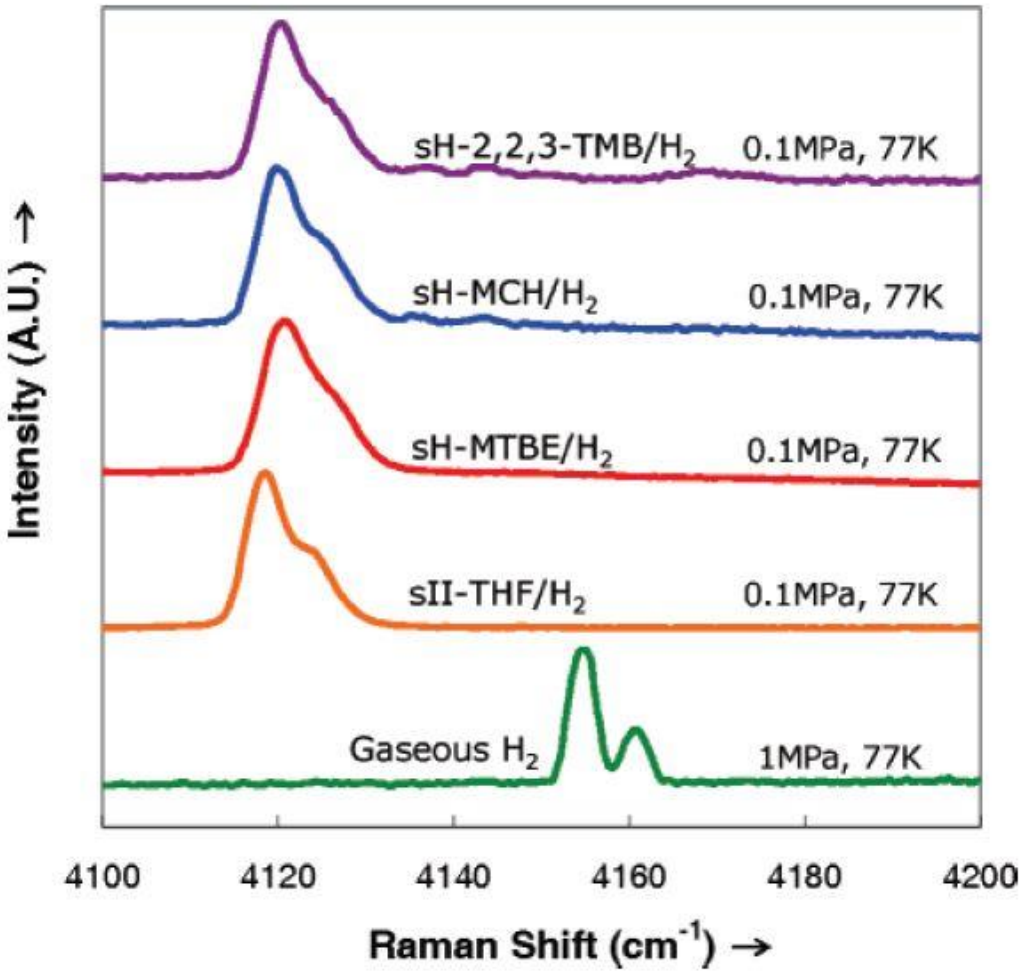

Figure 4.6: Raman vibrational spectrum for pure H2 gas, sII THF/H2 clathrate, sH MTBE/H2 clathrate, sH MCH/H2 clathrate, and sH 2, 2, 3-TMB/H2 clathrate. [14]

Strobel compared the Raman spectra for different sH hydrogen clathrates with Raman spectra for sII hydrogen clathrate in figure (4.6). This comparison showed that the vibrational peaks for both sH and sII clathrates are shifted to lower frequency than that of the free hydrogen molecules, which is logical due to the fact that hydrogen molecules have been enclathrated. Moreover, It can be noticed that the vibrational peaks for all sH clathrates are shifted from sII peaks by something like 1-2 cm^{-1}, which might be because a little difference in the cages size. As mentioned earlier, clathrates with sH structure trap hydrogen molecules into small 5^{12} cages, which is similar to the sII structure clathrates and would give same Raman peak, in addition to middle $4^3 5^6 6^3$ cages. In order to interpret the contribution of sH cages, the Raman spectra for sH clathrate was artificially red-shifted, which means that peaks from sH clathrate coincidence with peaks from sII THF/h_2 clathrate as shown in figure (4.7). [14]

From this comparison, there are two remarkable features; first of all, the shoulder existed in sII peak has been decreased in all sH peaks. Moreover, there is a noticeable broadening in all sH peaks. As the average radius of sH middle $4^3 5^6 6^3$ cage is only 0.1 Å, approximately, larger than the small 5^{12} cage, it is expected to have a superposition formed of Raman peaks for both cages. As a result of these facts, Strobel assigned the broadening in Raman peak for sH clathrates to contribution from middle $4^3 5^6 6^3$ cage, expecting to get also transitions Q_1 (1), and Q_1 (0). However, Strobel admit that experimentations with higher resolution are required to confirm his expectation of individual cage contribution. [14]

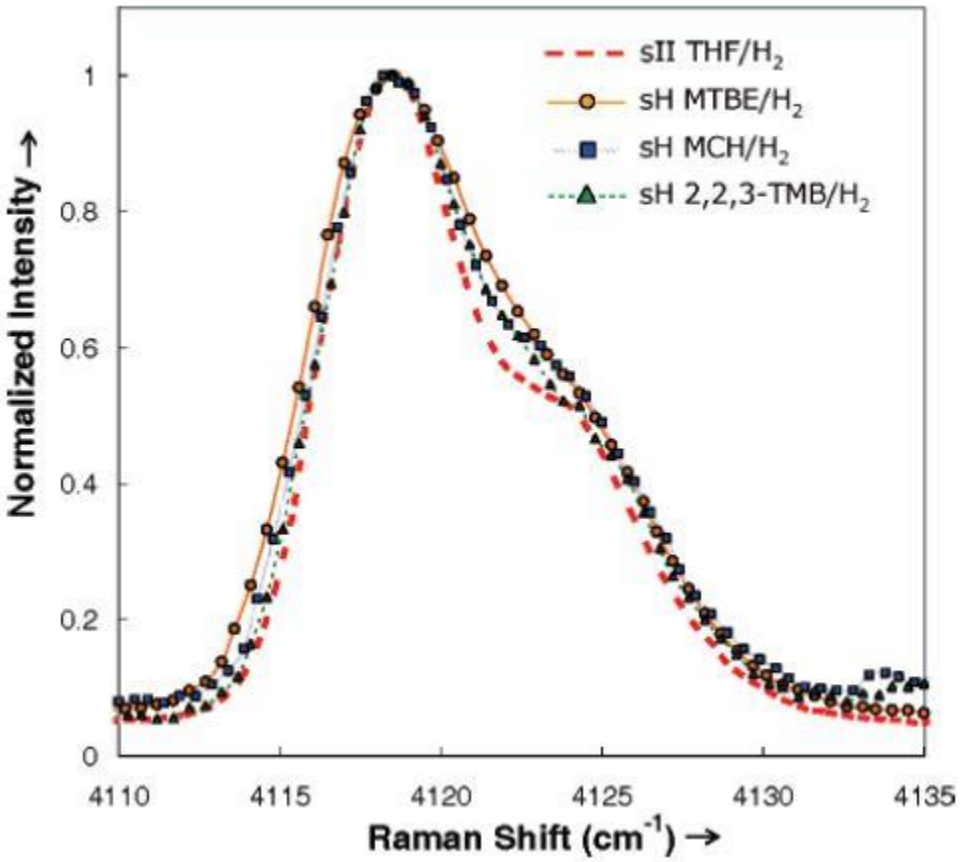

Figure 4.7: Vibrational Raman spectra for several sH clathrates and sII THF/H2 clathrate. sH clathrate spectra has been normalized (i.e. shifted -1 to -2 cm-1 to coincidence with sII spectrum. [14]

In addition, it was noted that the similar size of small 5^{12} cage and middle $4^3 5^6 6^3$ cage at sH structure, and the small frequency difference in Raman peaks of the two cages suggest that the middle $4^3 5^6 6^3$ cage can trap only one hydrogen molecule.

Chapter 5 OUR EXPERIMENT: A STUDY ON BINARY sH HYDROGEN AND DEUTERIUM CLATHRATES

According to the discussion carried out in the previous chapter, it is expected that the small 5^{12} cages and the middle $4^3 5^6 6^3$ cages can trap only one hydrogen molecule. This suggestion was reinforced by the fact that both cages have approximately the same size with a slight frequency difference between their Raman spectra. However, Strobel states that an additional experiment with higher resolution is required to confirm this estimation. [14] Consequently, an experiment of Raman spectroscopy has been performed to study binary sH MTBE/H_2 clathrate and MTBE/D_2 clathrate. In this chapter, some experimental details, such as the sample preparation, and equipment used, will be discussed. Then, results obtained by our team will be presented and discussed, in addition to data analysis. Finally, some comments and conclusion will be accounted.

5.1 Experimental Details

An ex-situ back scattering Raman spectroscopy experiment has been carried out to investigate binary clathrate hydrate in Raman Laboratory, Institute of Complex Systems (ISC) at National Research Center (CNR) in Florence, Italy. The binary sH MTBE/H_2 clathrate and MTBE/D_2 clathrate samples were initially prepared before performing the Raman spectroscopy.

5.1.1 Sample preparation

In order to prepare a MTBE/H_2 sH clathrate sample, crushed ice pieces (less than 250 μm) were placed in a high pressure stainless steel cell. After that, the ice particles were saturated with a large guest molecule (2.9 mol %) [14] The large guest molecule has been selected according to sH formation in well-studied systems with methane [20] including methyl tert-butyl ether (MTBE). Such clathrate sample was formed for a period of two days at pressure about 150 MPa and temperature about 275 K. [14] then, the sample was quenched into liquid nitrogen at temperature of 77K. Finally, the sample was kept at liquid nitrogen in order to prevent decomposition process due to higher temperatures.

For the other sample of MTBE/D_2 sH Clathrate, the same procedure has been followed, however, the ice pieces were replaced by heavy water (D_2o)

5.1.2 Equipment and experimental procedure

We have used a suitable cell that contains four slots that enables us to investigate different samples within the same cell as shown in figure (5.1). In order to switch the LASER beam between different slots, we use two pulleys attached to the arm containing the cell. One pulley is able to move the arm back and forth, while the other one moves the arm right and left.

To prevent LASER scattering before the sample, a transparent window is attached to the cell in order to effectively lead the LASER beam to the sample; for optimizing, the window should be cleaned first, and kept dry of any water drops in order to avoid ice formation on its surface during the cooling process, which might be an obstacle for the LASER beam. The cell has places for screws and screwdrivers to mount the cell in holder carefully. In addition, the cell is attached

to a cryogenic freezing device arm that enables us to change the temperature of the sample during the experiment. A closed cycle freezing cryostat has been used. After that, the whole arm including the cell is covered by a temperature incubator as shown in figure (5.2)

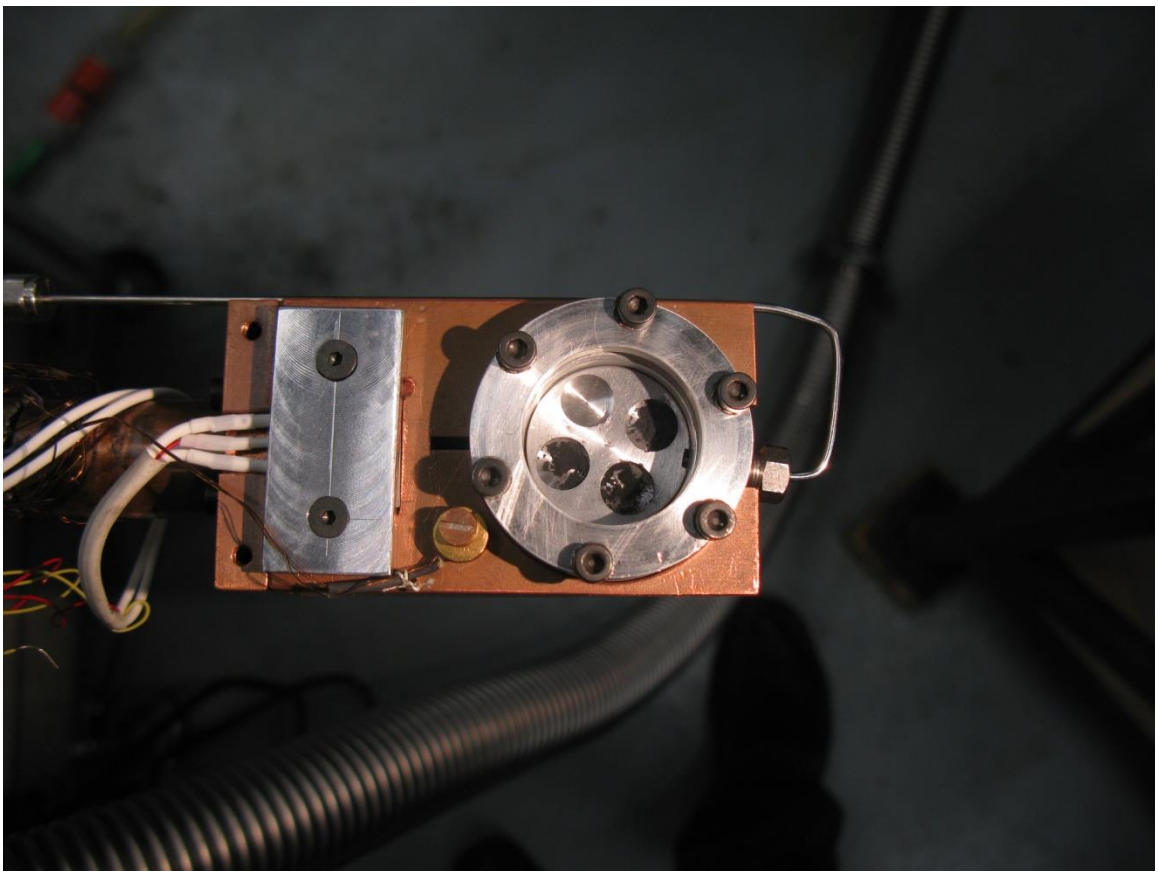

Figure 5.1: The cell that contains the sample; different slots for different samples at a time.

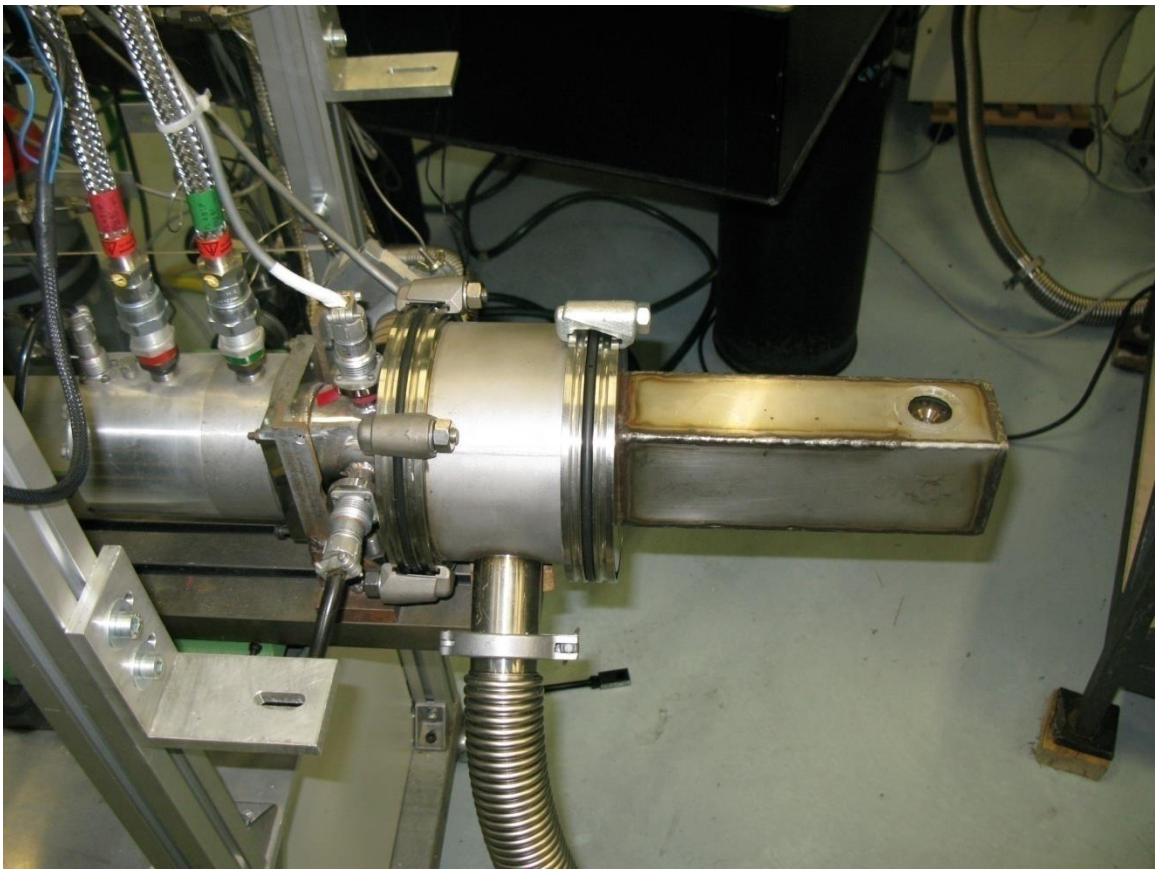

Figure 5.2: The cell is connected to the cryogenic freezing device arm.

The next step is to place the sample inside the cell in order to be able to perform Raman spectroscopy experiment. The previously prepared sample has been stored in liquid nitrogen tank to avoid clathrate decomposition. This means that we had to extract the sample from the tank and put it inside the cell. During this process, the sample is subjected to room temperature for short time. This rise in temperature threats the clathrate existence or at least might lead some of the guest molecules to escape from the clathrate compound. This temperature rise represents the main disadvantage of the ex-situ Raman experiment in which the sample is prepared away from the cell. In fact, the challenge is to decrease the time, as much as possible, between extracting the sample from the tank and placing it inside the cell. In addition, the ortho-para conversion process has already been occurred

during the sample storage, so that we expect to notice an equilibrium state achieved for the concentration ratio of both ortho and para.

In order to decrease the risk of decomposition due to room temperature during sample transferring and mounting processes, we used a shield around the cryogenic arm. This shield was full of liquid nitrogen, in contact to the cell, to keep the sample cooled during mounting the sample inside the cell. Moreover, gloves were attached to the shield, and they have been used to place the sample inside the cell.

After that, the cell has been closed using screws, and the shield with liquid nitrogen has been removed. The cell is now connected to the cryostat to control temperature of the sample. Moreover, silicon temperature sensors have been connected to the cell in order to observe temperature inside.

In order to perform Raman spectroscopy, An Argon Coherent-Innova 300C ion LASER has been used to produce a green LASER beam with wavelength equals to 5145Å. Figure (5.3) shows the LASER beam that comes out from the ion LASER source. The LASER beam has been guided through mirrors and then focused using lenses in order to let the beam incident at angle 90° on the cell window, and then incident on the sample. Figure (5.4) shows the configuration of lenses used to focus the LASER beam to the cell. Upon interaction between the LASER beam and the sample, back scattering beam has been collected by lenses to let it pass through spectrometer supported with a liquid nitrogen cooled charge coupled device CCD detector for the sake of data acquisition. Our team has been using Spex 1877 Triple monochromator with diffraction grating of 1800 g/mm (grooves per millimeter), while the Symphony II CCD detector, which is produced by Horiba scientific, has been used. Further explanation of CCD will be introduced in the appendix.

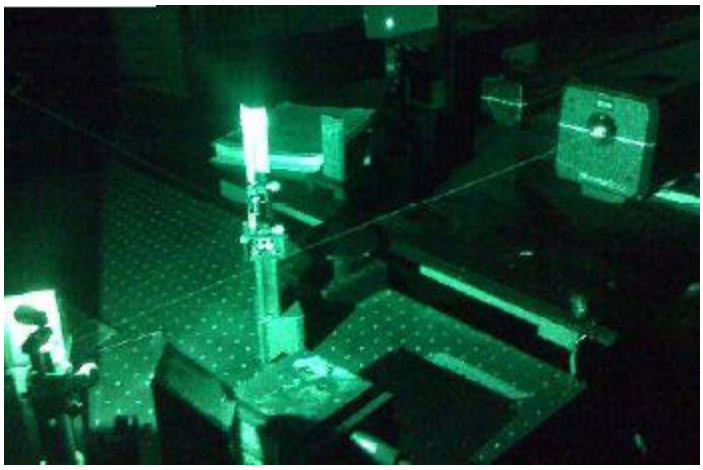

Figure 5.3: LASER beam produced by Argon ion LASER source.

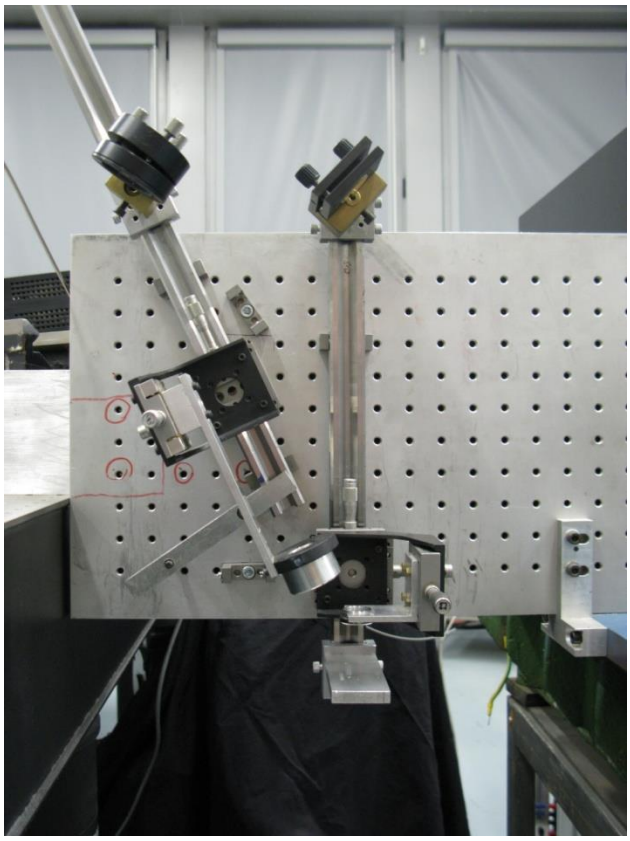

Figure 5.4: Configuration of lenses used to focus the LASER beam on the cell.

One of the problems that we have encountered is observing plasma lines associated with LASER beam. Such lines cause kind of interruption while analyzing Raman spectrum. As a result, we have removed such lines by using a diffraction grating in the path of LASER beam. Although plasma lines have been removed by this method, the grating has dispersed the LASER beam. As this dispersion dropped the signal off, some alignment for mirrors and lenses is needed to increase the signal once more. Consequently, we finally got fine Raman spectrum for the sample. Figure (5.5) shows the cell connected to cryogenic system with the cell exposed by the LASER beam.

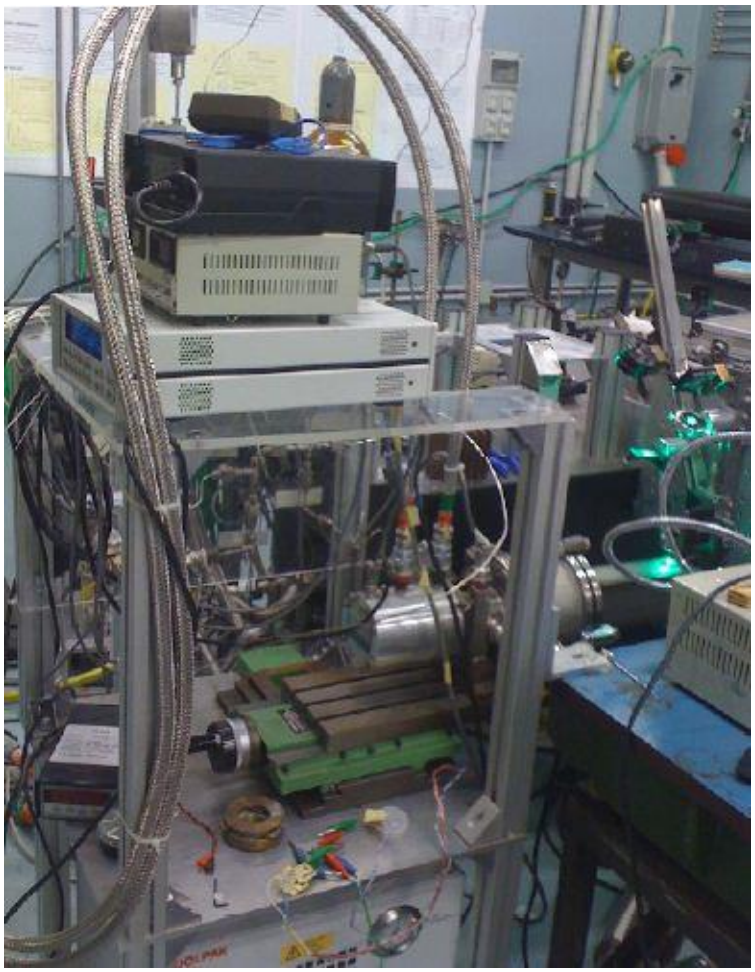

Figure 5.5: Cell connected to cryogenic system and is placed under the LASER beam.

Figure (5.6) shows the spectrometer used for our experiment and shows also the attached CCD detector attached to the spectrometer.

Figure 5.6: Spectrometer and the attached CCD detector.

5.2 Results and Data Analysis

Using the previously prepared sH MTBE/H_2 clathrate, and MTBE/D_2 clathrate hydrate, we performed high resolution Raman spectroscopy experiment through the equipment discussed above. Our team got Raman spectra for these samples, then the collected vibrational and corresponding rotational Raman spectra have been analyzed in order to investigate and confirm the occupancy of sH middle $4^3 5^6 6^3$ cage. In addition, heat cycles have been performed to the samples followed by another Raman measurement to observe the effect of temperature on the average occupancy.

As the sample was stored before the experiment, the ortho to para conversion process has been already occurred during the storage period. This means that the ratio of ortho to para has already reached the equilibrium state. In fact, the resulting spectra satisfied this expectation.

The collected spectra were fitted using Origin 8.6 Peak fitting module. Such fitting shows the individual contribution of molecules in each cage and how these contributions add up together in a way that gives the obtained results of Raman spectrum. For the sake of performing the fitting process, two main constraints have been used. First one is that all Gaussians should have the same full width at half maximum (FWHM), while the second constraint is regarding position of ortho and their corresponding para peaks. Indeed, the center of ortho peak is set to be about 6 cm^{-1} apart from the center of their corresponding para peak. As mentioned before, the difference of 6 cm^{-1} between ortho and para exists in case of free H_2 gas as well as clathrate hydrate, so we used this information to perform the fitting process. In addition, for deuterium, we used the constraint that the frequency displacement between $Q_1(0)$ and $Q_1(1)$ is ~ 2 cm^{-1} and between $Q_1(1)$ and $Q_1(2)$ is ~ 4 cm^{-1}.

Figure (5.7) shows the raw data for vibrational Raman spectrum of a previously prepared sample of binary MTBE/H_2 sH clathrate hydrate at temperature of 50 K before any heat treatment.

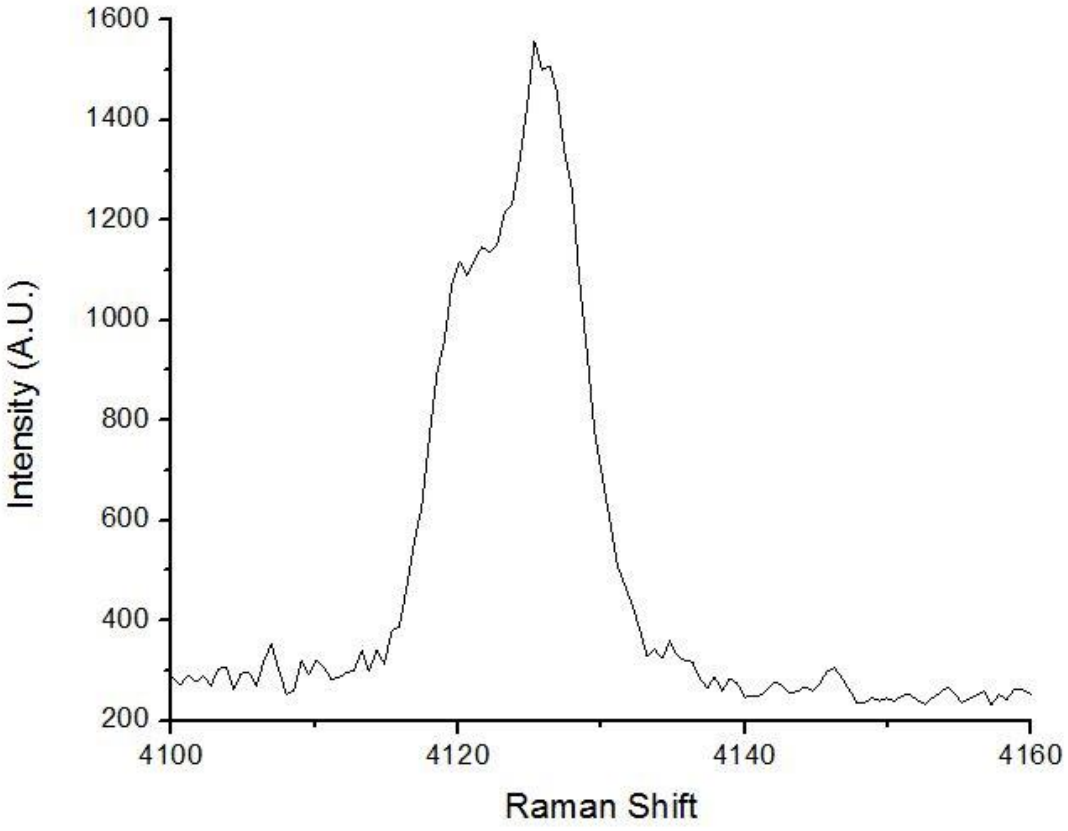

Figure 5.7: Raw data of the vibrational Raman spectrum of sH binary MTBE/H2 clathrate hydrate at temperature of 50K.

The result shows a broad curve that is due to contribution of hydrogen in both sH small 5^{12} cage and middle $4^3 5^6 6^3$ cage with frequency displacement between ortho and para peaks ~ 6 cm^{-1}. Taking strobel's results into consideration, it is noticeable that our equipment shows higher resolution which enables us to differentiate between ortho and para peaks for hydrogen in middle cage as well as in the small cage in a way that makes us sure about peak assignment.

Consequently, peak fitting process has been carried out for this raw data with position constraint applied on ortho and para peak for every single cage; which is 6 cm^{-1} difference, which means that the separation between every Gaussian has been set to be 6 cm^{-1}. In addition, the frequency difference between hydrogen in small cage and middle cage equals 1 cm^{-1}. This separation is applied between any two ortho peaks or any two para peaks. The outcome of this fitting process is shown in figure (5.8)

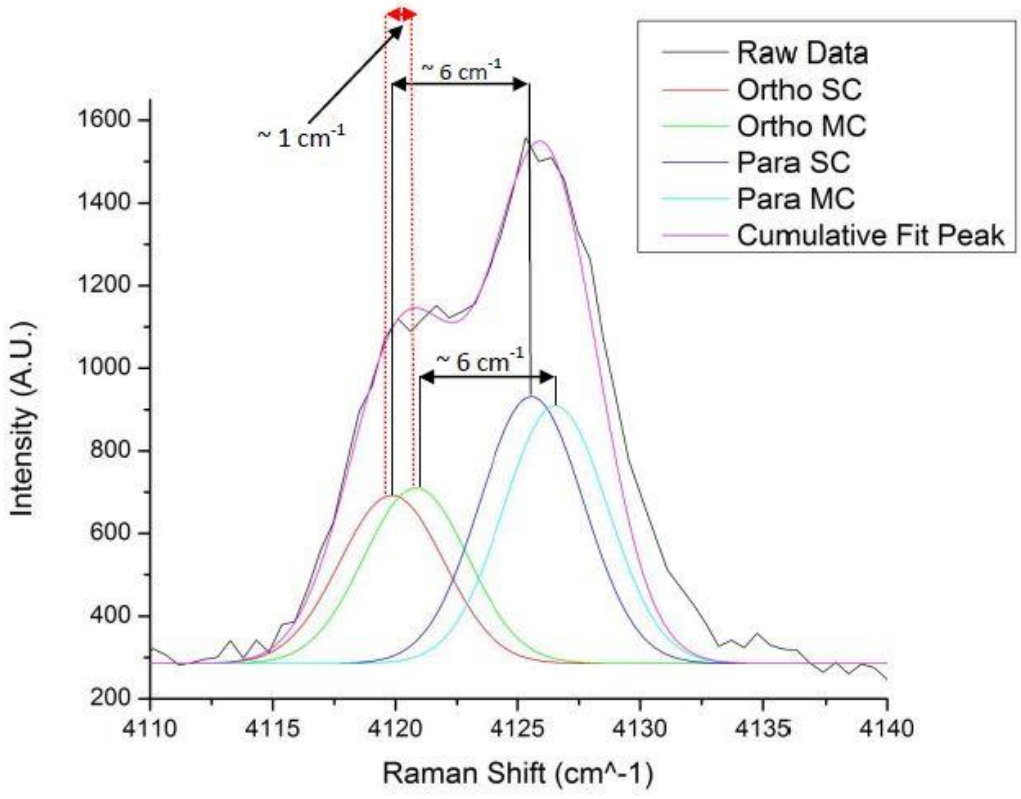

Figure 5.8: Fitted data of the vibrational Raman spectrum of sH binary MTBE/H2 clathrate hydrate at temperature of 50K.The constraint is that every Gaussian pair should be displaced by 6 cm^{-1}. And the difference between small and middle cage is 1 cm^{-1}

In the previous figure, ortho SC means orthohydrogen in the small 5^{12} cage, while ortho MC refers to orthohydrogen in the middle $4^3 5^6 6^3$ cage, and the same definition applies for parahydrogen in Small and middle cages. This fitting show explicitly that the middle $4^3 5^6 6^3$ cage in binary clathrate of sH structure can trap only one hydrogen molecule similar to the small cage, which confirms what Strobel expected using lower resolution equipment.

For further investigation, a heat treatment has been applied on the sample to witness the effect of temperature on the occupancy number for each cage in the binary clathrate hydrate. The temperature of the sample has been increased up to 100 K, and then the sample was quenched again to 50 K, and then Raman Spectroscopy measurement has been performed again. Figure (5.9) shows the raw data for vibration Raman spectrum.

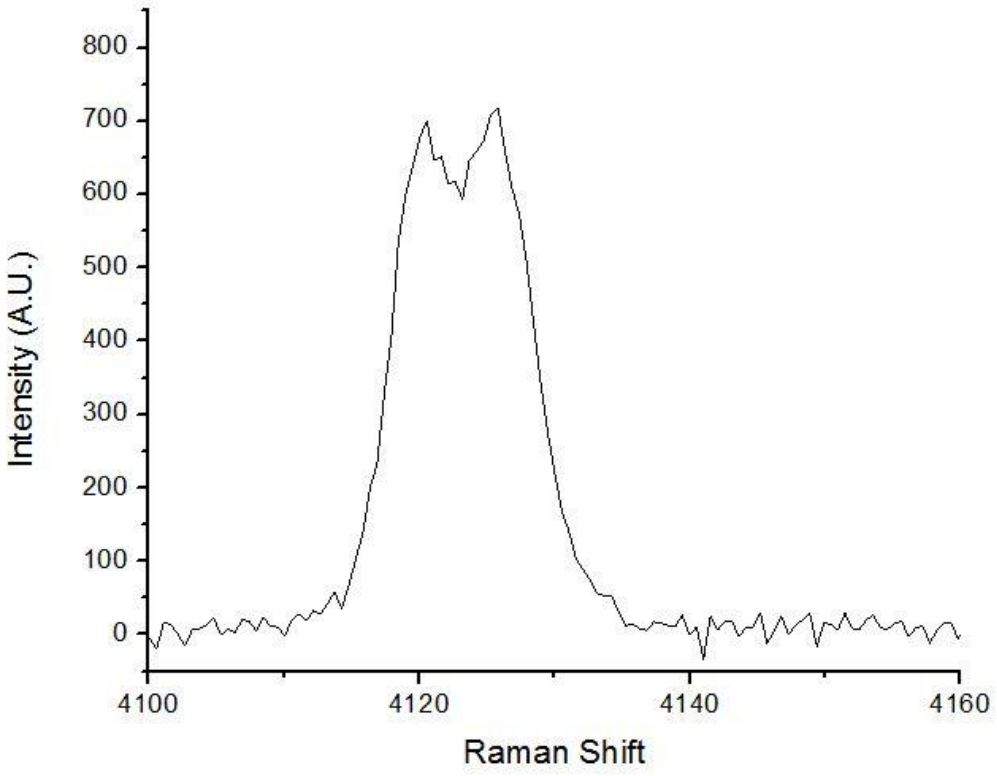

Figure 5.9: Effect of heat treatment on the vibrational Raman spectrum of sH binary MTBE/H2 clathrate hydrate at temperature of 50K after heating up to 100K and quenching back to 50K

According to figure (5.9), by performing one heat cycle on sH binary MTBE/H_2 clathrate hydrate lead the hydrogen molecule in the middle cage to escape. As a result of that, vibration Raman spectrum shows the ortho and para peaks of hydrogen molecule trapped in the small 5^{12} cage only.

Thus, fitting process has been done for orthohydrogen and parahydrogen in the small cage with constraint of frequency difference equals 6 cm^{-1}. The fitted data are given in figure (5.10)

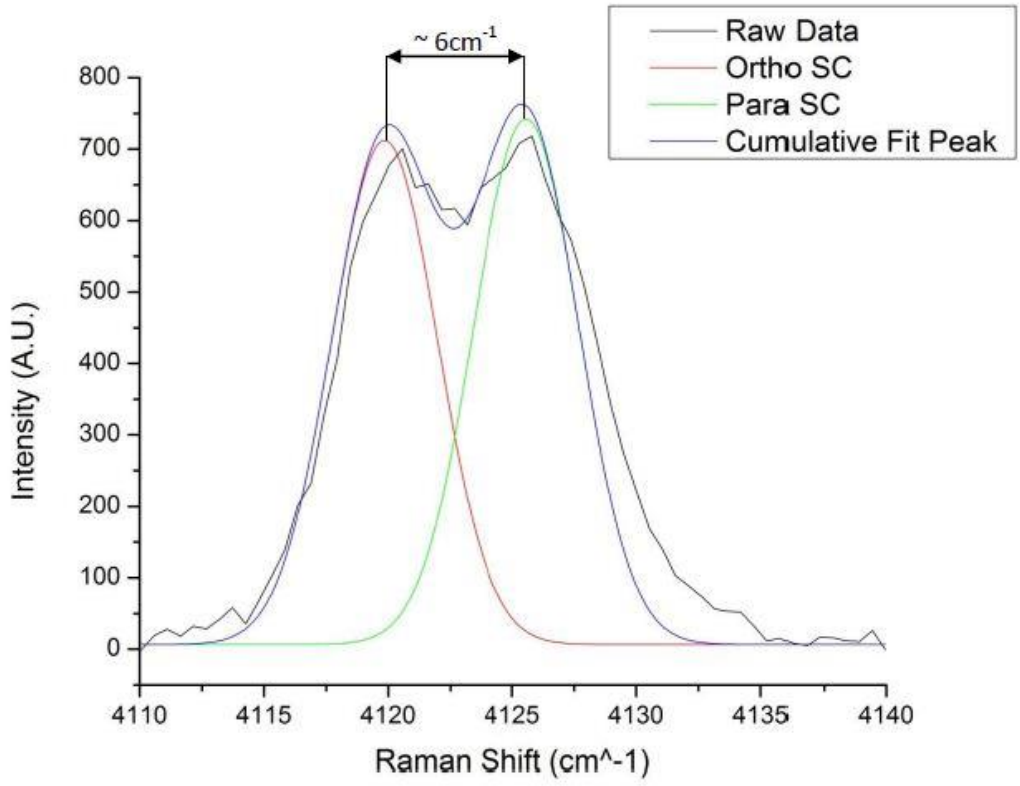

Figure 5.10: Fitted data shows the effect of heat treatment on the vibrational Raman spectrum of sH binary MTBE/H2 clathrate hydrate at temperature of 50K with constraint that every Gaussian pair should be displaced by 6 cm^{-1}.

So far, Raman spectroscopy for a previously prepared sample of sH binary MTBE/H_2 clathrate hydrate confirmed that the middle $4^3 5^6 6^3$ cage is occupied by a

single molecule of hydrogen as well as the small 5^{12} cage, and both cages are displaced by frequency equals to 1 cm^{-1}, while the large $5^{12}6^{8}$ cage is occupied by MTBE. In addition, performing heat treatment by increasing the temperature to 100K and then decrease it again down to 50K stimulates the hydrogen molecule in the middle cage to escape.

The other sample of sH binary MTBE/D_2 clathrate hydrate has been investigated by doing the same experiment once more. As mentioned earlier, the cell that we have used contains different slots for different samples, which enables us to perform Raman spectroscopy experiment on the other sample easily without dismounting the cell. Figure (5.11) shows the raw data for vibrational Raman spectrum of a previously prepared binary MTBE/D_2 clathrate hydrate at temperature of 50 K before any heat treatment.

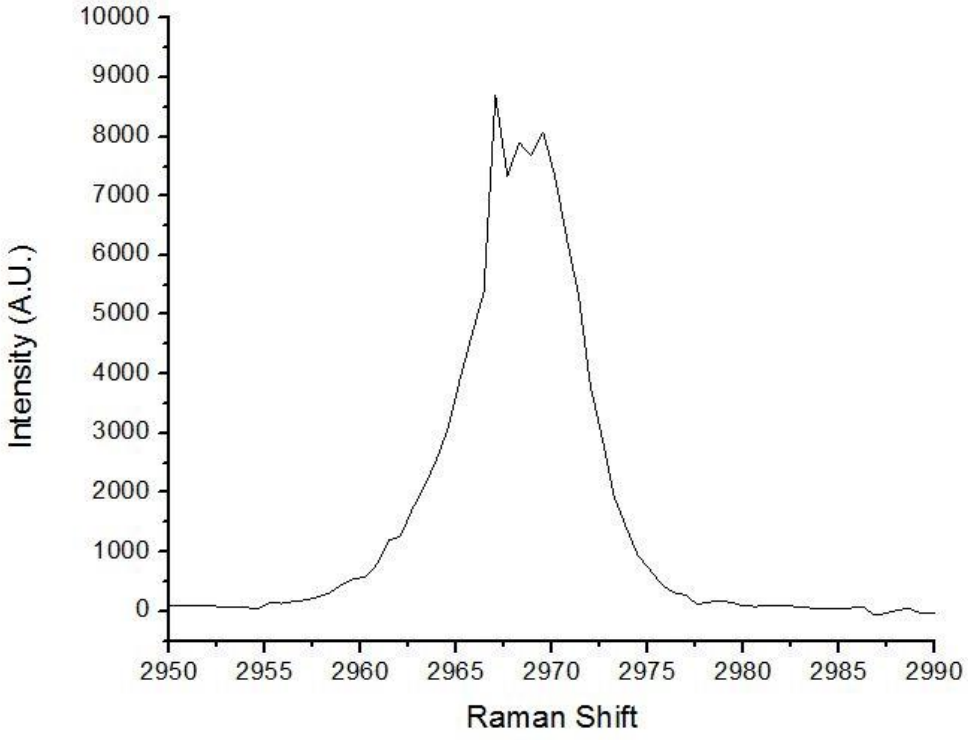

Figure 5.11: Raw data of the vibrational Raman spectrum of sH binary MTBE/D2 clathrate hydrate at temperature of 50K.

The resulting spectrum shows a broad curve, which implies that it has been resulted from contributions of small and middle cages. Unlike hydrogen, at 50K three vibrational transitions $Q_1(0)$, $Q_1(1)$, and $Q_1(2)$ are observed for deuterium because the corresponding rotational states are occupied at this temperature.

By analogy with what we did before, this spectrum has been fitted with the constraint implying that the displacement between $Q_1(0)$ and $Q_1(1)$ is ~ 2 cm^{-1} and between $Q_1(1)$ and $Q_1(2)$ is ~ 4 cm^{-1}. Moreover, the frequency difference between small cage and middle cage is 1 cm^{-1}. Figure (5.12) shows the result of this fitting process.

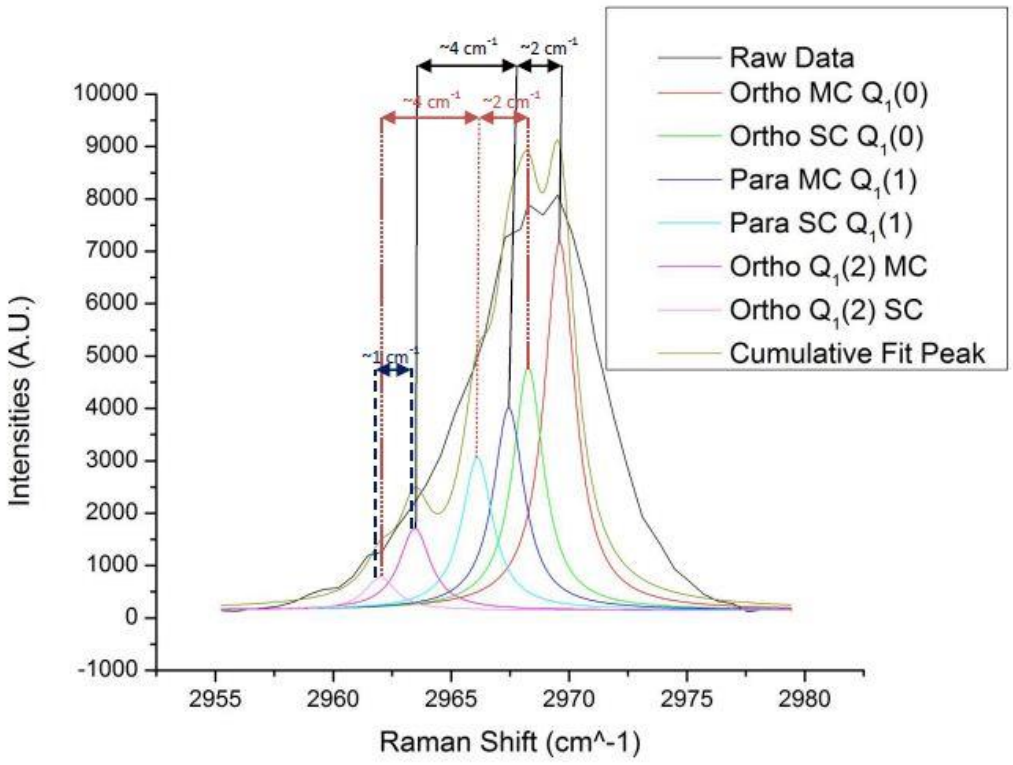

Figure 5.12: Fitted data of the vibrational Raman spectrum of sH binary MTBE/D2 clathrate hydrate at temperature of 50K.The constraint used is that the difference between $Q_1(0)$, $Q_1(1)$ is 2 cm^{-1} and difference between $Q_1(1)$ and $Q_1(2)$ is 4 cm^{-1}. And the difference between small and middle cage is 1 cm^{-1}

In the previous figure, SC refers to the small 5^{12} cage, while MC refers to the middle $4^3 5^6 6^3$ cage. Although deuterium is different than hydrogen as it contains three observable vibrational transitions at temperature of 50K, sH binary MTBE/D_2 clathrate hydrate is similar to MTBE/H_2 as the middle $4^3 5^6 6^3$ cage can trap only one deuterium molecule.

In order to confirm whether deuterium has the same behavior such as hydrogen or not, a heat cycle has been applied on the sample to observe the effect of temperature on the occupancy number for each cage. Like what have been done before, the temperature of the sample has been increased up to 100 K, and then the sample was quenched down to 50 K, and then Raman measurement has been performed once more. Figure (5.13) shows the raw data for the resulting vibration Raman spectrum after the heat cycle.

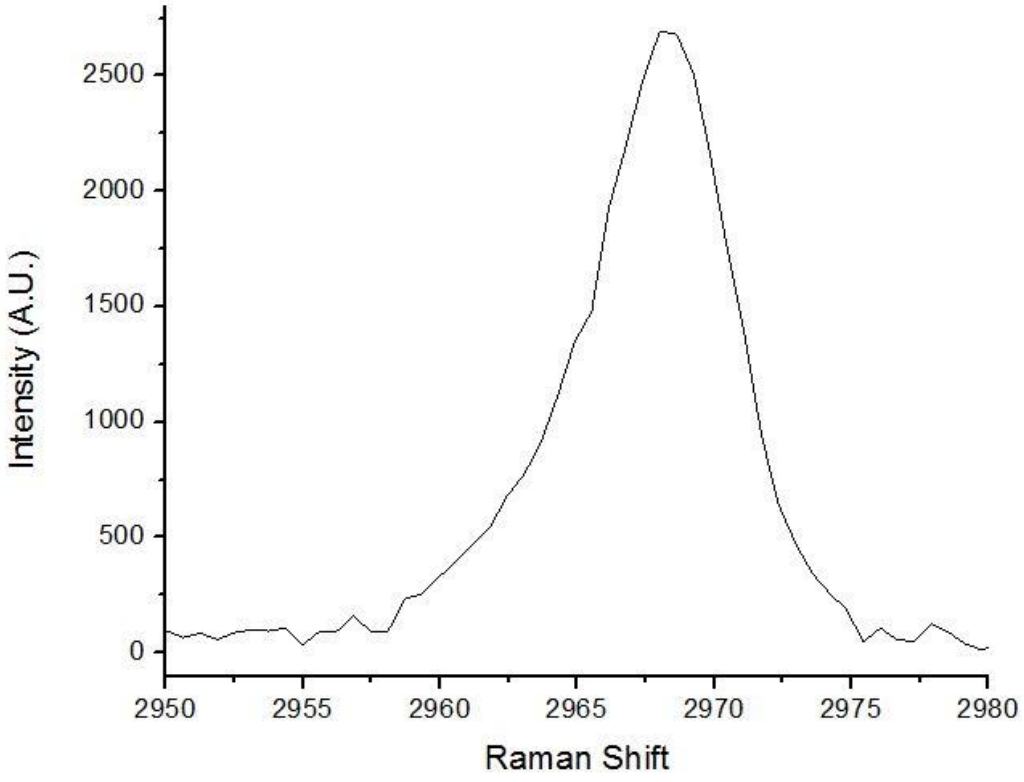

Figure 5.13: Effect of heat treatment on the vibrational Raman spectrum of sH binary MTBE/D_2 clathrate hydrate at temperature of 50K after heating up to 100K and quenching back to 50K

The previous figure shows a broad peak with a small shoulder to the left, in addition to the absence of ortho and para deuterium from the middle cage. This means that the heat treatment lead the deuterium molecule in the middle cage to escape due to increasing temperature, which is the same behavior noticed in case of MTBE/H_2. Moreover, the broad peak obtained refers to the existence of the deuterium molecule in the small cage. As a result of this, fitting process has been performed for the MTBE/D_2 after the heat cycle showing three vibrational transitions Q_1 (0), Q_1 (1), and Q_1 (2) for the deuterium molecule in the small cage. The fitted curve is given at figure (5.14)

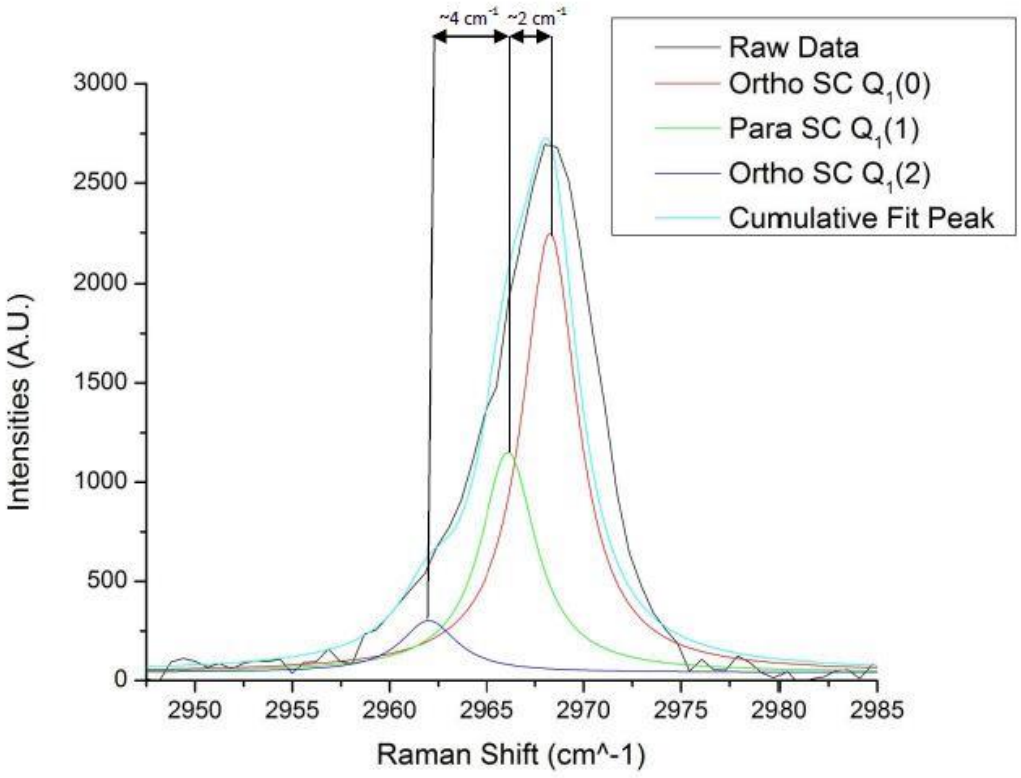

Figure 5.14: Fitted data shows the effect of heat treatment on the vibrational Raman spectrum of sH binary MTBE/D_2 clathrate hydrate at temperature of 50K. The constraint used is that the difference between Q_1 (0), Q_1 (1) is 2 cm^{-1} and difference between Q_1 (1) and

Thus, the fitting curve for MTBE/D_2 binary clathrate after one heat cycle shows that deuterium has the same behavior like hydrogen as the heat treatment forced the deuterium molecule in middle cage to escape. However, the deuterium molecule trapped in small cage is still there even after the heat cycle.

5.3 Conclusion

The problem under consideration for investigation is the occupancy number for small 5^{12} cages and middle 5^{12} 6^{8} cages of the binary sH clathrate hydrate. While it was already well known that the large cage would be occupied by a large guest molecule such as MTBE for stability issues, it was suggested in previous research that middle cage can trap only one hydrogen molecule, however, this assignment was in need to be confirmed using high resolution equipment. Thus, our team performed Raman spectroscopy experiment to confirm the assignment of single occupancy number for middle cage.

Binary sH MTBE/H_2 clathrate hydrate sample in addition to binary sH MTBE/D_2 clathrate hydrate samples have been previously prepared at CNR, Italy. Our team investigated these previously prepared samples using high resolution Raman spectroscopy to reveal the occupancy number of middle cage. Consequently, the collected data of vibrational Raman spectrum has been fitted using Origin 8.6 Peak fitting module with specific constraints for hydrogen as a guest molecule and for deuterium. The basic constraint is that the orthohydrogen is displaced from parahydrogen by frequency equals 6 cm^{-1}, while for deuterium, the difference between first and second transitions is 2 cm^{-1}, and the difference between second and third transition is 4 cm^{-1}.

The resulting curves confirmed clearly that the middle 5^{12} 6^{8} cage in sH structure is occupied by one hydrogen molecule such as the small 5^{12} cage. The same experiment was performed with deuterium and the same result was encountered such as the case for hydrogen. Subsequently, heat treatment has been applied by

performing heat cycle (i.e. heating up and quenching). It was remarkable that increasing temperature force the single molecule trapped in the middle cage to escape, while single molecule in small cage was still there. This breaking down is because that molecule in middle cage has frequency more than that for the molecule in small cage. In other words, our high resolution equipment confirmed what was expected for sH middle 5^{12} 6^{8} cage.

APPENDIX A

VIBRATIONAL – ROTATIONAL ENERGY TRANSITIONS

In rotational and vibrational spectroscopy, specific letters are used to express ΔJ transitions in rotational quantum numbers. The letters P, Q R, S are used to express shift in rotational quantum number by values -1, 0, 1, 2 respectively. As Raman spectra for a diatomic molecule has a selection rule of $\Delta J = 0, \pm 2$ the spectrum will include Q and S branches. Thus, the transition $S_{\Delta v}(J)$ means that the molecule initially at rotational state J and then undergoes a shift in rotational quantum number by value of $\Delta J = 2$, while Δv is the change in vibrational states. Consequently, $S_0(1)$ refers to a pure rotational transition starts at J=1 and shift to J=3 with no vibrational transition. In addition, the transition $Q_{\Delta v}(J)$ means the molecule undergoes shift in vibrational states while keeping rotational states unchanged. Consequently, $Q_1(1)$ refers to a molecule initially at vibrational $v=0$ and J = 1, and then undergoes vibrational transition to $v = 1$ with no change in rotational quantum number. Figure (A) shows an example for the vibrational-rotational transitions.

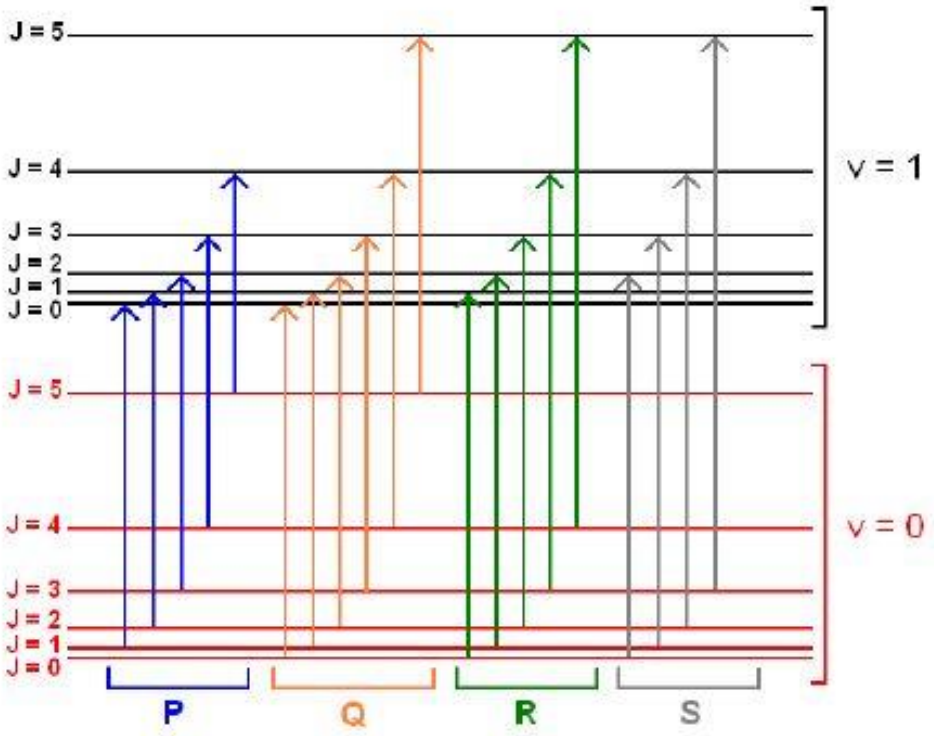

Figure A: Vibrational – rotational energy transitions. [6]

APPENDIX B

CHARGE - COUPLED DEVICE (CCD)

The Charge – Coupled Device (CCD) is used as a light detector. It is simply an integrated circuit (IC) detects light signals and able to store and display such signals. The process occurs by converting the incident photon into an electrical charge with an electrical charge intensity corresponding to the color of each pixel. The conversion process is conducted using a p-doped Metal-oxide semiconductor Capacitor (MOS). Figure (C) shows schematic diagram for the internal structure of the CCD.

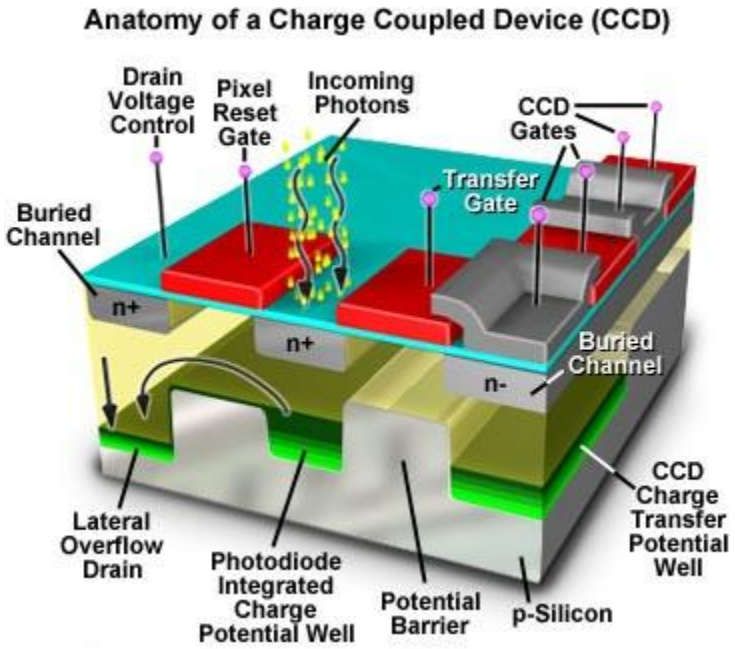

Figure B: CCD internal structure. From Hamamatsu photonics [21]

REFERENCES

[1] Oxford dictionaries.

[2] Strobel, T.A ; Hester, K. C; Koh, C. A; Sum, A. K. and Sloan, J. E. D; "Properties of the Clathrates of Hydrogen and Developments in their Applicability," Chem. Phys Lett. 2009, 4-6, 97-109.

[3] Dyadin, Y. A., Larionov, E. G., Aladko, E. Y., Manakov, A.Y., Zhurko, F, V,. Mikina, T .V .,Komarov, V .Y ., and Grachev, E .V. "Clathrate Formation in Water-Nobel Gas (Hydrogen) Systems at high pressure", J , Struct. Chem. 1999, 40, 790-791.

[4] Retrieved on May 2013 from Los Alamos National Laboratory Website http://www.ees.lanl.gov/ees6/clathrates/

[5] Long, D., " The Raman Effect: A Unified Treatment of the Theory of Raman Scattering by Molecules," 2002.

[6] Zaghloul, M. A., Study of the Raman Spectrum of Simple Clathrate Hydrates of Hydrogen, M.Sc thesis, Faculty of Engineering, Cairo University, 2011.

[7] Strobel, T. A., On Some Clathrates of Hydrogen, PhD thesis, Colorado School of Mines, 2008.

[8] Strobel, T. A.; Sloan, E. D. and Koh, C. A.; "Raman spectroscopic studies of hydrogenclathrate hydrates," J. Chem. Phys. 2009, 130, 014506.

[9] Holder, G. D.; Stephenson, J. L.; Joyce, J. J.; John, V. T.; Kamath, V. A. and Malekar, S.; "Formation of clathrate hydrates in hydrogen-rich gases," Ind. Eng. Chem. Des. Dev. 1983, 22, 170.

[10] Minzhong, X.; Sebastianelli, F.; Bačić, Z.; Lawler, R. and Turro, N. J. ; "H2, HD, and D2 inside C60: Coupled Translation-Rotation Eigenstates of the Endohedral Molecules from Quantum Five-Dimensional Calculation," *J. Chem. Phys.* 2008, 6, 064313.

[11] Lokshin, K. A. and Zhao, Y. S.; "Fast synthesis method and phase diagram of hydrogen clathrate hydrate," *Appl. Phys Lett.* 2006, 13, 131909.

[12] Duarte, A. R. C.; Shariati, A.; Rovetto, L. J. and Peters, C. J.; "Water Cavities of sH Clathrate Hydrate Stabilized by Molecular Hydrogen: Phase Equilibrium Measurements," *J. Phys Chem B,* 2008, 7, 1888.

[13] Dyadin, Y. A.; Larionov, E. G.; Manakov, A. Y.; Zhurko, F. V.; Aladko, E. Y.; Mikina, T. V. and Komarov, V. Y.; "Clathrate hydrates of hydrogen and neon," *Medeleev* Commun. 1999, 5, 209.

[14] Strobel, T.A ; Koh, C. A; and Sloan, J. E. D; " Water Cavities of sH Clathrate Hydrate Stabilized by Molecular Hydrogen" J. Phys. Chem. B 2008, 112, 1885-1887.

[15] Lokshin, K. A.; Zhao, Y.; He, D.; Mao, W. L.; Mao, H.-K.; Hemley, R. J.; Lobanov, M. V.; Greenblatt, M. Phys. ReV. Lett. 2004, 93, 125503.

[16] Strobel, T. A.; Taylor, C. J.; Hester, K. C.; Dec, S. F.; Koh, C. A.; Miller, K. T.; Sloan, E. D. J. Phys. Chem. B 2006, 110, 17121.

[17]Hester, K. C.; Strobel, T. A.; Sloan, E. D.; Koh, C. A. J. Phys. Chem. B 2006, 110, 14024.

[18]Udachin, K.; Lipkowski, J.; Tzacz, M. Supramol. Chem. 1993, 3, 181.

[19] Anderson, R.; Chapoy, A.; Tohidi, B. Langmuir 2007, 23, 3440.

[20] Ripmeester, J. A.; Ratcliffe, C. I. J. Phys. Chem. 1990, 94, 8773.

[21] Retrieved on July 2013 from Hamamatsu photonics official website.

http://www.hamamatsu.com/us/en/index.html

[22] Giannasi, A.; Celli, M. and Ulivi, L.; "Low Temperature Raman Spectra of Hydrogen in Simple and Binary Clathrate Hydrates," J. Chem. Phys. 2008, 8, 084705.